

Explaining and replies to the comments and suggestions

Ms. Ref. No.: cp-2017-50

Title: Environmental dynamics since the last glacial in arid Central Asia: evidence from grain size distribution and magnetic properties of loess from the Ili Valley, western China

Following parts are our explanations what changes to the manuscript have made and how our replies (Answer or Reply, A&R, Black) to the reviewer's comments ([comments and suggestions, C&S, Blue](#)).

Replies to the comments of Dr. Vandenberghe

For *General Comments*

C&S: Many studies deal with the correspondence between loess deposits and climate circulation but the causal relations are indeed poorly understood. Previously, the attention has been drawn to competing circulation systems of westerlies and monsoons. Thus, relations are indeed best studied in a region where different systems could have been present at times. Consequently, the studied region is favorably situated for this timely research. A most interesting result is the importance of precipitation on the loess depositional signal. Until now most attention has been paid to temperature variability that of course also impacts the wind circulation. It seems by this study that resulting oscillations in loess deposition show a complex pattern. And this may be the reason for the fact that the oscillating loess signals in C. Asia and the NE Tibetan Plateau are not that simply correlated with D-O-events or H-events. The paper is well written, designed and archived.

A&R: Thanks for your positive comments. This paper made aims to investigate the causal relations between loess deposits and climate circulation. Recently, many researchers have paid much attention to paleoclimate reconstruction in transitional regions where different atmospheric systems predominate at different times, e.g. the Central Balkans (Ramisch et al., 2016), the Qinghai Lake region (Cheng et al., 2012), southwest Asia (Hamzeh et al., 2015). Our study area is likewise situated in the zone influenced by different climatic systems. It therefore becomes important prerequisite to clarify the paleoenvironmental significance of various proxies, in particular which proxies reflect temperature, which represent precipitation, and which indicate wind strength. Our manuscript explores the potential impacts of precipitation on the loess depositional signal, and identifies areas where more work needs to be done in the future.

We agree that some scientists have focused on the influence of temperature variability on wind circulation, and in particular the role of local insolation minima in driving an early onset of the LGM in the Southern Hemisphere (Vandergoes et al., 2005). We reconsider the reasons for variations in EM1 proportions, and suggest that the availabilities of source sediments which are likely impacted by development of permafrost and vegetation growth in dust source areas, are responsible for the weaker EM1 proportion fluctuations in LGM and early-MIS3. Please see the details in line 464-470 and 504-509 of revised manuscript. The aeolian loess sediments in Central Asia are more likely to respond to a complex mixture of global signals with local insolation, glacial activity and local weathering. This overlap will weaken the global signals as preserved within the loess.

For *Minor Comments*

C&S: L 343-359: Two different explanations are claimed for the origin of the fine-grained endmember 3 (c. 18.9 μm). The main difference seems to be, if I understand well, that one hypothesis invokes high-suspension transport while in the other one surface winds are involved. However, both hypotheses interpret that this component is the result of background loess supply (as confirmed in lines 389-395) as previously demonstrated by Prins et al (2007), Vriend et al (2011) and Zhang et al (1999). It is not realistic to separate the grain-size fractions of 2-8 μm (transported by westerlies) and 8-15 μm (=EM3, transported at low altitude) as the authors seem to do. Both components react jointly constituting background loess supplied by westerlies as described by e.g. Prins et al. (2007).

A&R: We agree with the reviewer on this point. The origins of the EM3 size fraction is indeed complex. For example, based on modern dust monitoring from the high-altitude subtropical Puna-Altiplano Plateau in South America, Gaiero et al. (2013) found that “Finer mode dust is deposited during event periods, which point to a dominant long-range transport, contrasting with a dominance of coarser mode observed for non-dust sampling periods, pointing to dominant local sources.” Prins and Vriend (2007) and Prins et al. (2007) suggested that the clayed loess component represented the fine dust component supplied over the entire Loess Plateau by long-term suspension processes, and the high-level subtropical jet stream (westerly winds) might, at least partly, be responsible for the input of this fine-grained loess component. End-member unmixing results of Xiaerbulake (XEBLK) loess (Li et al., 2016b) grain-size distributions show the similar EM3 component to NLK loess (Fig. R1). XEBLK loess section is also located in the Ili Basin. That implies that the fine-grained EM3 (c. 18.9 μm) is the result of background loess supply in the Ili Basin regardless of its origin (Vriend et al., 2011; Zhang et al., 1999; Prins et al., 2007). It is difficult to determine the origins of the fine silt/clay. The appearance of the fine component in dust deposition may be caused by aggregation, due to fine particles adhering to the coarse particles, as well as chemical weathering. Perhaps the method of Machalett et al. (2008) is the better alternative. They neither removed organic matter and carbonates from the stratigraphic samples and nor applied an intensive ultrasonic treatment to disaggregate particles.

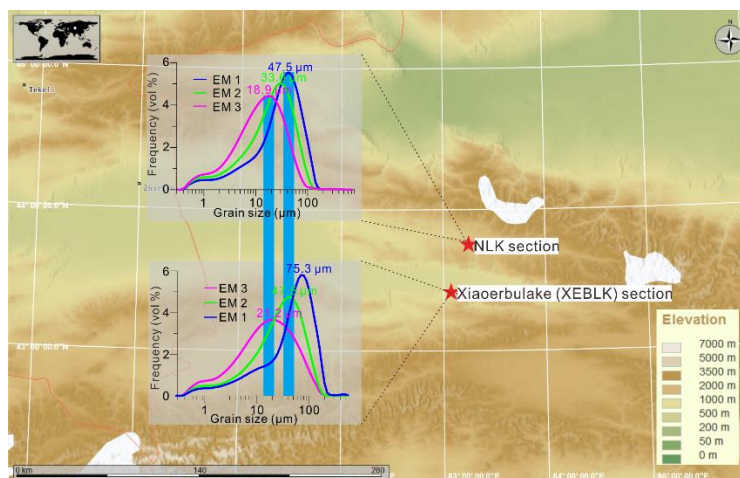


Fig. R1 Comparison of end-member unmixing results of NLK loess and Xiaerbulake (XEBLK)

loess grain-size distributions.

C&S: L 441-447: If the Ili valley is sheltered from northeastern wind, as the authors claim, what is then the source area for the EM1 and EM2 fractions? There is no apparent difference between these coarse-grained fractions on the CLP, N Tibet Plateau and in the Ili valley where a distinct supply is clear from the northeast under the influence of the Siberian High.

A&R: Thank you for this suggestion. The northern Tien Shan Range reaches altitudes of > 4000 m a.s.l. For the particles with grain size of > 20 μm , it is unlikely that grains of this coarser silt fraction were transported by north-easterly winds above the 4000 m altitude over the northern Tien Shan and into the Ili Basin. We therefore interpret the coarser grained loess particles in the Ili Basin to have been predominantly transported by near-surface winds. The topographic context (Fig. 1 in revised manuscript) most likely ensured the westerly winds coming to be the transporting agent. Moreover, we added modern meteorological data (2009-2013) in NLK in the *Supplementary file*. It was evident that the strongest winds at NLK site mainly blowed from the west.

In our speculation as to the provenance of the NLK loess, we initially compared the REE parameters of NLK loess with those of desert sands and modern soils from the Ili Basin and further west into Kazakhstan (Fig. R2). Our results indicated that the deserts and topsoils in Kazakhstan are unlikely to be the main potential source areas. In contrast, topsoils from the Ili Basin probably provide the most important source materials in the NLK loess. The Quaternary sediments of the Ili Basin mainly consist of alluvial fans and floodplains, and the top soils developed on those. We therefore speculate a proximal source for the NLK loess. Furthermore, recent work from our group indicates that size-differentiated rare earth elements (REE) may help to distinguish potential proximal or distal sources (Chen et al., 2017). In future, we expect to find more substantial evidence for tracing loess provenance in the region.

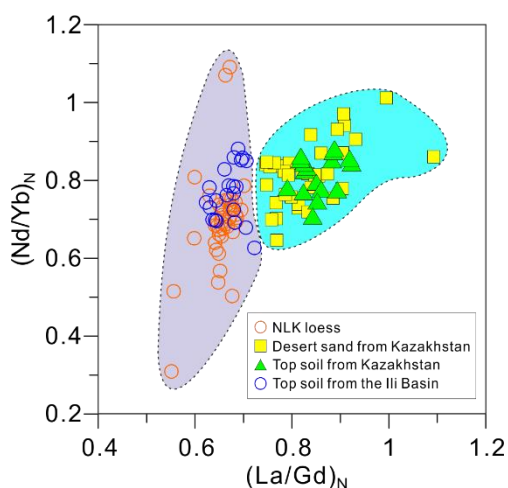


Fig. R2 (Nd/Yb)_N vs. (La/Gd)_N of loess, top soil and desert sands from the Ili Basin and Kazakhstan.

C&S: L 454-456: Explain better how the ‘cyclonic storms’ originated by protrusion of the Arctic polar front, rather than by other circulation patterns.

A&R: This is a constructive question. We have reconsidered this issue. We have collected some modern and Holocene records about atmospheric circulation in Central Asia over the past month,

and exclude the influences of the Arctic polar front and assure the importance of the Siberian High for dust transport and increased loess accumulation at NLK.

Available data enable us to compare our data from the eastern, sheltered end of the Ili Basin with the Remisowka section at the southwestern margins of the basin – with respect to likely climatic influence and its impact on grain size. Remisowka (Machalett et al., 2008) is located along the northern piedmont of Tianshan Mountains (Fig. 1a in manuscript). Because NLK site is much more sheltered from northerly weather systems than Remisowka, there is a good chance that the polar front had more of an influence on Remisowka than on NLK. While in the north/northeast of our study area is a massive cold high — Siberian High. The Siberian High is the most dominant Northern Hemisphere anticyclone and is centered between 40°N and 65°N, 80°E and 120°E (cf. Fig. 3 in Huang et al. (2011)), and its anticyclonic feature is broadly recognized as the dominant mode of winter and spring climate over Eurasia (Sahsamanoglou et al., 1991; Savelieva et al., 2000; Panagiotopoulos et al., 2005; Gong and Ho, 2002). In addition, based on modern and Holocene climate data, we argue that the Siberian High may have exerted a significant influence on wind dynamics in the Ili Basin, leading to dust transport and the accumulation of loess during cold phases in NLK.

In addition, modern meteorological data show that the maximum wind at NLK mainly blows from the west, and that dust storm development in Ili river valley is closely linked with southward-moving high-latitude air masses, while the air masses can enter into the Ili Basin round the northern Tianshan (see the Fig. S5 in *Supplementary file* and Ye et al. (2003)). Therefore, the Siberian high-pressure system is able to influence the Ili Basin, and the southward-moving high-latitude air masses associated with it can enter into the Ili Basin, leading to dust transport and the accumulation of loess deposits during cold phases in NLK.

Also, we compare secular trends between the EM1 proportions and mean grain size data from the Jingyuan section over the last glacial period (Sun et al., 2010). It is widely accepted that increases in grain-size records from the CLP are linked to a strengthening of the East Asian winter monsoon due to an intensification of the Siberian High (Hao et al., 2012; Ding et al., 1995). The similarities in the trends can be observed (Fig. 7 in revised manuscript). For example, there remain coarser grain size and higher sedimentation rate during mid-MIS3 (Sun et al., 2010), and opposite cases occur in early- and late-MIS3. Therefore, that supports that a common Eurasian atmospheric forcing pattern — the Siberian High — is responsible for the climate evolution of these two regions during that time period. Therefore, we have rewritten the section 5.3. Please see *Lines 439-487* in the revised manuscript.

C&S: L 476: The interesting absence of correlation between the observed grain-size signals and N Atlantic abrupt events is not only found in the Ili valley but also previously in Tadjikistan and the NE Tibet Plateau (Vandenberghé et al. 2006)

A&R: That point has been attracting the attention of our group recently. We find that EM1 proportions fluctuate weaker in H2 and H5 events (Fig. 7 in the revised manuscript). We thus reconsider the reason for variations in EM1 proportions, and suggest that the availabilities of source sediments which are likely impacted by development of permafrost and vegetation growth in dust source areas, are responsible for the smaller EM1 proportions in LGM and early-MIS3. Please see the details in line 464-470 and 504-509 in the revised manuscript.

Therefore, in our view, the lack of good correlation between observed grain-size and millennial-

scale Atlantic events suggests that the loess records in Central Asia represent a response not only to global signals but also local signals, such as glacial activity and local weathering. This overlap will weaken the global signals.

C&S: L 483-484: This sentence is not clear: is ‘which’ referring to the conclusions by the authors or by Vandenberghe et al.? It is not clear therefore what really is contradicting

A&R: I am so sorry for the poor expression. The ‘which’ referred to the conclusions by the authors. We have revised the sentence, like this “Darai Kalon is located in a region where the mid-latitude westerlies clearly have a much stronger influence, especially during full glacial conditions (Vandenberghe et al., 2006). In contrast, our results from the Ili Basin suggest that the mid-latitude westerlies did not always predominate north of the Kyrgyz Tian Shan due to northward or southward movement of the climate subsystem. In this case, the high mountains in Central Asia most likely obstructed the migration of the Asiatic polar front further south towards Tajikistan where those data were derived (Machalett et al., 2008), thereby resulting in a stronger westerlies signal at Darai Kalon than at NLK.” The movement northward or southward of mid-latitude westerlies makes the Ili Basin more sensitive to paleoclimate change in Central Asia, which establishes the strategic position of the Ili Basin in paleoclimatic reconstruction.

However, as we mentioned above, the Siberian high-pressure systems predominate in the Ili Basin during cold phases, leading to dust transport and increased loess accumulation at NLK, and our grain-size proxy data can also correlate with abrupt events, such as Heinrich events (H1 to H6) identified from the North Atlantic records, though EM1 proportions fluctuate weaker in H2 and H5 events. Therefore, we have revised this section.

For Technical comments

C&S: L 123: ‘more reliable’ than what?

A&R: Thank you for your careful reading. We have rewritten this sentence. Actually, we mean that the optically stimulated luminescence (OSL) dating is more reliable for constructing a loess chronology than AMS ¹⁴C ages for older than MIS2 aeolian sediments according to Song et al. (2015).

C&S: L 317: ‘shorter’ than what?

A&R: EM1 is likely derived from shorter distance transport of suspended load owing to its larger modal grain size. Thus, its transport distance is shorter than the finer grains, like the EM2 and EM3 fractions in this manuscript.

C&S: L 139: insert ‘were’ between ‘S1’) and ‘then’; Figure 1 is too small.

L 182: remove ‘are’;

L 513: remove ‘can’ or ‘may’.

A&R: Yes, these are grammar errors. We have corrected these mistakes accordingly. We also

adjusted the layout of Fig. 1 and increased front size. Thank you.

C&S: I suggest to shorten the title a bit

A&R: Yes, we have rewritten the title, “Aeolian dust dispersal patterns since the last glacial period in eastern Central Asia: Insights from a loess-paleosol sequence in the Ili Basin”. Thank you.

C&S: Dear authors, I agree with most of your replies and thank you for the modifications. I just want to react with 2 comments: 1. To the origin of the very fine silt-clay component: Chemical weathering is indeed a good candidate as measured by Konert and Vandenberghe 1997, and well-illustrated by the experiments of Sun YB et al 2006. Transport as aggregates of fines by monsoonal dust storms (Qiang et al 2010) is contradicted by their very widespread and general occurrence (Vandenberghe 2013). Adherence of fines to larger grains has been contradicted by several authors. 2. Provenance of EM 1-2: I agree with your explanation. I understand now that you also agree with a northern wind, however not crossing the high mountains to the north but carrying dust only at low elevation over short distance. In my opinion, the carrying agent may still be the northern monsoonal wind, although restricted to the Ili basin.

A&R:

1. The complexity of finer component is reflected in not only its origin but also uncertainty of instrument measurement (Ujvari et al., 2016; Mason et al., 2011). Chemical weathering can efficiently decrease grain size of loess (or paleosol) through the transformation of feldspar minerals into clay minerals linked closely to the process of pedogenesis. Sun et al. (2011) regarded this component formed by pedogenesis “ultrafine component”. However, we have investigated clay mineralogy of NLK loess section, and the results show that the major clay mineral components in the NLK section were illite, chlorite, kaolinite and smectite, and that those clay minerals mainly had detrital origin, and rather than are in-situ weathered products. Moreover, variations in illite contents along the NLK section may be controlled by wind intensity, because weaker wind intensity would transport more fine fractions, which was supported by the wind tunnel experiment (Wang et al., 2017). Therefore, we think the degree of influence of chemical weathering on the loess grain size depends on the differences of environment conditions from site to site. Qiang et al. (2010) suggested that formation of aggregation increased particle mass, which enabled fine grains to be deposited even under stronger winds by dry deposition, however, the aggregates had larger pores and relevant lower density than individual mineral grain of the same size. Therefore the aggregates still can be influenced by the effects of sorting by aeolian processes. However, by observing the dust deposition collected in dust storm, Lin et al. (2016) thought that particles less than 20 μm could settle down during floating dust weather when the wind velocity decreased and even stopped. Therefore, it seemed to be difficult to distinguish that the aggregates were formed after deposition or they were transported by winds directly. Observations of modern dust under the scanning electron showed the phenomena of aggregation and/or fine particles adhering to larger ones (Pye, 1995, 1987; Derbyshire et al., 1998; Falkovich et al., 2001; Qiang et al., 2010), whereas the micrographs of fresh samples from the southern margin of Tarim Basin under SEM showed little aggregation, or adhering of fine particles to the coarse particles (Lin et al., 2016). Maybe more convincing evidence will come from a lot of studies of modern storm processes.

2. Yes, we agree with you. After reconsideration as mentioned above, we suggest that the Siberian high-pressure system exerts a significant influence on wind dynamics and thus the loess deposition in the eastern Ili Basin. Therefore, we have rewritten the section 5.3. Please see *Lines 439-487* in the revised manuscript.

Replies to the comments of anonymous Referee #2

For *Linguistic issues*

C&S: Lines 37-42: A lack of correlation between EM1 proportions and GISP $\delta^{18}\text{O}$ values at the millennial scale, combined with modern weather data, suggests that Arctic polar front predominates in the Ili Basin and the Kyrgyz Tian Shan piedmont during cold phases, which leads to the dust transport and accumulation of loess deposits, while the shift of mid-latitude westerlies towards the south and north controls the patterns of precipitation/moisture variations in this region. Reviewer's note: a lack of correlation between A and B means C was dominant? It implies that there are no other possibilities (D, E, ...). Even worse, is "while the shift of the mid-latitude westerlies ... controls patterns of precipitation/moisture ..." corresponding to or with "shift of the Arctic polar front controls the temperature patterns of wind strength"? If so, you have to say so.

A&R: Thanks for your critical comments. The logic of the abstract was unclear, and it is unreasonable to draw conclusions beyond the information available in the data. We have now tried to clear the confused logic, and rewritten the Abstract and Conclusions sections in this manuscript. It is important to note that Central Asia is very large and consequently it is reasonable to assume that different climate subsystems act upon different parts of the region. Therefore, observations made at one end of Central Asia (e.g. Tajikistan) do not necessarily apply to the other (e.g. Ili Basin). Furthermore, the Ili Basin itself is almost 1000 km across and is geographically diverse, and it is reasonable to assume that the western part of the basin, e.g. the published site of Remizovka, is more exposed to influences such as the polar northerlies than sites in the eastern part of the basin, e.g. NLK presented here, which are much more sheltered by the high Tien Shan mountains.

Tajikistan is mainly impacted by the westerlies, and the North Atlantic climatic signals are presented in Tajikistan loess, which implies that the westerlies linking the North Atlantic and the Eurasia loess, can influence accumulation of loess deposits in Tajikistan (Vandenberghe et al., 2006). A lack of good correlation between EM1 proportions and GISP $\delta^{18}\text{O}$ values at the millennial scale only indicates that other climate systems control the wind dynamics responsible for dust transport and the accumulation of loess during cold phases in NLK, rather than the Westerlies. Thus, we cannot conclude that "Arctic polar front predominates in the Ili Basin and the Kyrgyz Tian Shan piedmont during cold phases."

We added some records from modern and Holocene climate change records to substantiate our arguments for mid-Westerlies changes. Actually, those records demonstrated that the mid-latitude Westerlies truly controlled the patterns of moisture variations in Arid Central Asia (ACA) (Huang et al., 2015; Li et al., 2011b; Cai et al., 2017). However, we can't draw that conclusion from "A lack of correlation between EM1 proportions and GISP $\delta^{18}\text{O}$ values at the millennial scale".

"while the shift of the mid-latitude westerlies ... controls patterns of precipitation/moisture ..." isn't corresponding to or with "shift of the Arctic polar front controls the temperature patterns of wind

strength”. Available data enable us to compare our data from the eastern, sheltered end of the Ili Basin with the more exposed Remizovka section at the southwestern margins of the basin – with respect to likely climatic influence and its impact on grain size. Remisowka (Machalett et al., 2008) is located along the northern piedmont of Tianshan Mountains (Fig. 1a in manuscript). Because NLK is much more sheltered from northerly weather systems than Remisowka, there is a good chance that the polar front had more of an influence on Remisowka than on NLK. Furthermore, based on modern and Holocene climate data and comparison of the EM1 proportions and mean grain size (MGS) data from the Jingyuan section in northwestern CLP, we argue that the Siberian High may have exerted a significant influence on wind dynamics in the Ili Basin, leading to dust transport and the accumulation of loess during cold phases in NLK. Therefore, we argue that the Siberian High controls wind strength and mid-latitude westerlies control precipitation/moisture. A strengthened Siberian High would push the mid-latitude Westerlies pathways further to the south, resulting in comparably drier conditions in the northern Central Asia regions (e.g. Tianshan Mountains) but wetter conditions in south-western Central Asia (Pamir) (Lei et al., 2014; Wolff et al., 2017). Intensity and geographical position of the Siberian High can strongly control precipitation and atmospheric circulation patterns (meridional or zonal) at mid-latitudes of Asia (Panagiotopoulos et al., 2005). The coupling of the Siberian High with the mid-latitude Westerlies system likely contributed significantly to the climate variability in the study area. We have modified our text to explain these drivers more clearly, and also rewritten the *Abstract*. Please see details in the revised manuscript

C&S: Lines 42-44: Comparison of EM1 proportions with Northern Hemisphere summer insolation clearly illustrates local insolation-based control on wind dynamics in the region, and humidity can also influence grain size of loess over MIS3 in particular. Reviewer’s note: to me (this reviewer), the logic relationship between these two sentences are not traceable at all. “local insolation-based control on wind dynamics”: what does this mean?

A&R: We reconsider the relationships between June insolation at 45°N and EM1 proportions in Fig. 7, and the reasons for variations in EM1 proportions. We think it is more reasonable to consider that the availabilities of source sediments which are more likely impacted by development of permafrost and vegetation growth in dust source areas, are responsible for the weaker EM1 proportion fluctuations in LGM and early-MIS3. Therefore, we have deleted the discussion of summer insolation. Please see the details in line 464-470 and 504-509 of revised manuscript.

C&S: Lines 55-60: The relative influence and intensity of these major climate subsystems have varied across the latitudinal and longitudinal range of Central Asia through time. Thus identification of the predominant climate regimes in a certain region is a crucial precondition for tracing paleoclimatic evolution. Reviewer’s note: (1) relative influence? Maybe relative importance. (2) The first sentence continues its SPECIFIC tone (i.e., Central Asian), but the second sentence turns to a general tone (i.e., a certain region). To me (this reviewer), it is misleading.

A&R: (1) We have clarified this distinction in the text, and substituted “relative influence” with “relative importance”. (2) We cannot use a specific concept to represent a general concept. It is indeed misleading. We have changed the second sentence to “Thus identification of the predominant

climate regimes in this region, using geological archives, is a crucial precondition for tracing paleoclimatic evolution.”

C&S: Lines 66-72: While loess in Central Asia has (.....) increasingly formed the focus of loess research, as yet the forcing mechanisms and the climatic conditions responsible for loess-paleosol sequences formation are ambiguous, and the paleoclimatic evolution recorded by these loess deposits in this region is not systematically understood. Reviewer’s note: to me (this reviewer), “increasingly formed the focus”, “the forcing mechanisms ... are ambiguous”, and “not systematically understood” are all belong to “expression inadequacies”.

A&R: Here, we have simplified the language and made the purpose of this paper much clearer and better to understand. We also added three citations in an effort to reinforce the lack of systematic understanding of the forcing mechanisms and the climatic conditions responsible for loess-paleosol sequences formation.

C&S: Lines 78-81: Climatic teleconnections, especially between the North Atlantic and East Asian Monsoon regions, are likely to have been recorded within the Central Asian loess. As yet, however, the region so far largely lacks data by which the role and contribution of the central parts of the Eurasian continent, as an environmental bridge, can be elucidated. Reviewer’s note: to me (this reviewer), there is a logic gap in this statement. I mean that you (authors) may have to bring the environmental bridge to the front so that the importance of Central Asia in documenting the teleconnections is pronounced first.

A&R: Thanks for your suggestion. We have clarified the language in the text and the wording of our arguments. Since we know basically nothing about millennial-scale climatic changes in Central Asia, our aim is to investigate a loess section in Central Asia to see to what degree climatic teleconnections exist between North Atlantic and East Asia first, i.e. the first step is to generate data. Therefore, we have made the aim clearer, like this “Data for Central Asian loess are so far lacking at this resolution, despite its strategic location as a likely environmental bridge between the North Atlantic and East Asian Monsoon regions.” We deleted the sentence “Climatic teleconnections, especially between the North Atlantic and East Asian Monsoon regions, are likely to have been recorded within the Central Asian loess.”

C&S: Other suggestions Magnetic Susceptibility 1.1. “Low susceptibility in paleosols and high susceptibility in loess units” were sufficiently documented in Alaskan loess and in Siberian loess and Professor Liu Xiuming is a leading scientist on this. Please see if his works and propositions can help you. 1.2. The coarse particle-association of high susceptibility can be tested simply by measuring the susceptibility of different particle size fractions. This can be done on selected samples and the data of the selected samples may elevate your confidence of interpretation. 1.3. If I were the author, I would have completely excluded susceptibility portion from this paper and may (just may) write a separate paper on magnetic susceptibility.

A&R: The relationship between pedogenesis and magnetic susceptibility in the higher-latitude loess deposits of Alaska and Siberia is different from the Chinese Loess Plateau loess as suggested by Liu

et al. (1999) and Liu et al. (2008). At NLK, lower susceptibility exists in paleosols and higher susceptibility in loess units. Although this scenario is difficult to explain fully through variation in wind strength alone, it showed that wind strength, or wind dynamics, would influence MS variations at least and thus paleoclimatic reconstruction using climatic proxies, such as MS. Thus it is necessary to understand the atmospheric dynamic pattern during loess deposition further.

Consistently low $\chi_{fd}\%$ values in both loess and paleosol layers demonstrated that the content of SP particles is very low, and consequently that their contribution to MS can be ignored. That is, weaker pedogenesis prevents the efficient production of SP grains. We hence consider that alloegenetic magnetic minerals made the greater contributions to MS, and these correlate with dust transportation. Following the reviewer's suggestions, we sieved five samples into $> 63 \mu\text{m}$, $63 - 40 \mu\text{m}$, $40 - 32 \mu\text{m}$, $32 - 20 \mu\text{m}$ and $< 20 \mu\text{m}$ grain size fractions, and each of samples were measured at least three times using a Bartington MS2 meter. Our results showed lower MS values in $> 63 \mu\text{m}$ grain size fractions and maximum values existed in $32 - 20 \mu\text{m}$ or $< 20 \mu\text{m}$ grain size fractions (Table R1), which indicated that the major ferromagnetic minerals were always smaller than sand size. Therefore, we deleted the sentence "MS enhancement at NLK is primarily driven by increased concentrations of sand-sized detrital magnetic minerals" in the manuscript.

Understanding the mechanisms for the enhancement of magnetic susceptibility is beyond the scope of this study. We only intended to illustrate the significant impacts of wind dynamic on MS. In addition, ferromagnetic minerals, including magnetite and hematite, belong to heavy minerals which have higher relative density. Thus when wind becomes stronger, more ferromagnetic minerals will be transported to deposition areas, resulting to higher MS values. Thus we have modified the subtitle 5.1, like this "Impacts of wind strength on magnetic susceptibility variations".

Table R1 Magnetic susceptibility values ($10^{-8}\text{m}^3\text{kg}^{-1}$) of different grain-size fractions

Sample No.	Grain-size Fractions				
	$> 63 \mu\text{m}$	$63-40 \mu\text{m}$	$40-32 \mu\text{m}$	$32-20 \mu\text{m}$	$<20 \mu\text{m}$
NLK400	72	66	86	88	98
NLK800	67	61	80	87	85
NLK1108	73	78	104	107	108
NLK1110	75	68	96	109	105
NLK1400	79	83	94	100	111

Note: Red font represents maximum values in different grain-size fractions.

C&S: Particle Size 2.1. You need a comprehensive and streamlined review on existing literature dealing with interpretation of loess particle size. The literature review can be either "school division-based" or time-based (earlier time and later time) or country based (west and China). **2.2.** After the expected review is properly done, you may delete those insignificant references (I mean that you cited too many and that many of them may be insignificant). **2.3.** Since you heavily rely on Vandenburghe (2013) for EM1, EM2, and EM3 arguments, you are strongly suggested to provide a complete and concise re-statement of Vandenburghe (2013) in debating pros and cons of EM1, EM2, and EM3 for representing aolian dynamics. If he was so sure and nobody else was at his odd, your application of EM1, EM2, and EM3 to interpreting aolian dynamics may be more acceptable. If his argument was case-dependent, you have a harder task to establish your case though. **2.4.** I am wondering if the cumulative particle-size curve does show a statistically meaningful break between EM1 and EM2 and also a break between EM3 and EM2? If it does not, should your reliance on

Vandenberghe (2013) be questionable? What I try to say is: if you can confidently justify the acceptance of EM1, EM2, and EM3 for representing aeolian dynamics, you do have a case here. Otherwise, your opponents can always argue that: those coarse particles may have indeed locally sourced, but those fine particles can either be remotely (high-elevation) sourced or locally (near-surface) sourced.

A&R: Thanks for your suggestions. In the section 5.2, we have summarized the significance of grain-size analysis. Relevant studies were separated into two groups according to the unmixing method of grain size spectra. Vandenberghe (2013) applied visual inspection of grain-size distribution curves and the EMMA end-member analysis in combination to define the characteristic grain-size distribution of primary loess deposits and review their respective processes and conditions of transports and deposition, relying largely on loess samples from central and eastern Asia and northwestern and central Europe. Thus his argument was based on a large number of previous studies from a range of sites, and is not case-dependent. For example, *the subgroup 1.b.2* in Vandenberghe (2013) has also been identified in the loess of Chinese Loess Plateau, southern, northwestern and central Europe. Furthermore, in the studies of loess sediments from the Qilian Mountain region, Rasmussen et al. (2014), Nottebaum et al. (2015) and Yang et al. (2016) have interpreted the multiple sources of loess sediments and dynamic conditions according to sediment groups in Vandenberghe (2013). We have included those arguments in the main text.

EM1 and EM2 of our results have modal grain size approximately corresponding to the ‘*subgroup 1.b.1*’ and ‘*subgroup 1.b.2*’ respectively. Vandenberghe (2013) suggested that although component 1.b.1 and 1.b.2 occur jointly together in the proximal depositional regions, they are clearly distinct from each other in terms of the coverage and transportation distance. In Fig. 4 of manuscript, the mirror image relationships over millennial scales can be observed, which may implied that both EM1 and EM2 have a same origin, but wind strength controlled the relative proportions of both through time. In addition, grain-size distributions of modern dust illustrate a modal grain size of 33.3 μm in winter and 44.6 μm in summer in the northern and western Chinese Loess Plateau (Sun et al., 2003) (Fig. R3). These modes are similar to EM2 and EM1 in our results, respectively. It is generally assumed that vegetation coverage is more extensive in summer than in winter in CLP. Therefore, availability of sediments in source areas wouldn’t influence the grain sizes, conversely differences in wind dynamic between these two seasons likely play an important role in controlling the grain sizes. While EM3 (“*subgroup 1.c.1*”) indicated a different aerodynamic environment from EM2. The former would settle when the wind velocity decreases and even stops, as suggested by Lin et al. (2016), but the latter were interpreted as transportation during cyclonal dust storm outbreaks (Vandenberghe, 2013). Consequently, the cumulative particle-size curve can give a statistically meaningful break between EM1 and EM2 and also a break between EM3 and EM2.

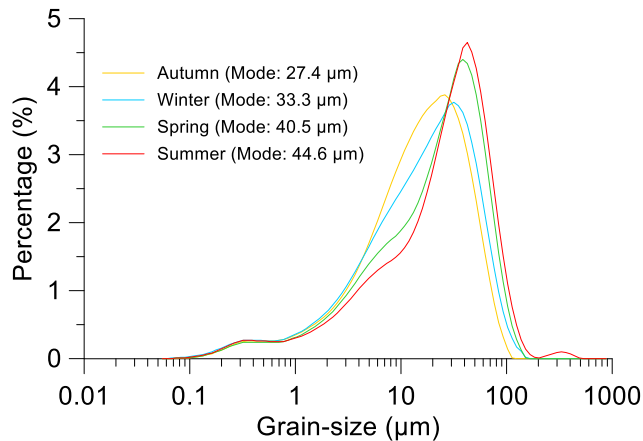


Fig. R3 Grain-size distributions of seasonal dusts in the northern and western CLP (Huanxian) Actually, greater dispute exists in the origin of the EM3 size fraction. In the manuscript, we suggest that the fine-grained EM3 (c. 18.9 μm) is the result of background loess supply in the Ili Basin, and infer the EM3 modal peak to derive from low altitude non-dust storm processes after excluding the aggregate model, transportation by high-altitude westerlies and influences of post-depositional processes. Therefore, those fine particles are also likely to be locally (near-surface) sourced.

C&S: Questions for 5.3 Aeolian dust dynamics in eastern Central Asia: links to atmospheric systems
 Lines 440-447: Central Asia is variably influenced by the Asian monsoon from the south (Dettman et al., 2001; Cheng et al., 2012), the mid-latitude westerlies (Vandenberghe et al., 2006), the Siberian high-pressure systems from the northeast (Youn et al., 2014), and the polar front from the north (Machalett et al., 2008). However, by virtue of its geographical position, most of these climate influences can be excluded for the Ili Valley since it is sheltered to the northeast, east and south. The Asian high mountains largely inhibit the intrusion of Asian (Indian and East Asian) monsoons to the region, and the influence of the Siberian High (An, 2000) has been shown to decrease westward from the CLP (Vandenberghe et al., 2006). Reviewer's note: Downplaying Asian monsoons may be acceptable since the Yili Valley is indeed blocked by the Tianshan Mountains on the south. But, downplaying Siberian high-pressure system (SibH) is not well justified. Yes, SibH is weakening away from its center, but you cannot say that the Yili Valley was beyond the SibH influence. Furthermore, your favored "polar front" is actually also blocked by high mountains on the north. If polar front was indeed the major player, you may have to provide modern climate backgrounds in which strong polar front interacted with the prevailing westerly flow to stimulate dust storms in the Yili Valley.

A&R: Thanks for your good suggestions. As described above, the Siberian high-pressure systems predominate in the Ili Basin during cold phases, which leads to dust transport and increased loess accumulation at NLK, and the mid-latitude Westerlies controlled broad-scale patterns of moisture variation across ACA.

Modern meteorological data show that the maximum wind at NLK mainly blows from the west, and that dust storm development in Ili river valley is closely linked with southward-moving high-latitude air masses, while the air masses can enter into the Ili Basin round the northern Tianshan (see the Supplementary materials and Ye et al. (2003)). Therefore, the Siberian high-pressure system is able to influence the Ili Basin, and the southward-moving high-latitude air masses associated with it can

enter into the Ili Basin, leading to dust transport and the accumulation of loess deposits during cold phases in NLK. The coupling of the Siberian High with the mid-latitude Westerlies system likely contributed significantly to the climate variability at NLK in the eastern Ili Basin.

We have rewritten the section 5.3. Please see the details in the revised manuscript and Supplementary materials.

C&S: Lines 448-456: Modern satellite data indicates that dust storm development in Ili river valley is closely linked with southward-moving high-latitude air masses (Ye et al., 2003). Karger et al. (2016) provided a detailed picture of the westerlies for the Ili Basin, in which a rain belt gradually migrated towards the south and north in autumn and summer, respectively. According to this scenario, enhanced evaporation coupled with strengthened westerly winds would bring more humid and warm air masses to Arid Central Asia (ACA) during the Holocene (Zhang et al., 2016). Therefore, based on our grain-size observations, we argue that the Arctic polar front, intruding southward in the winter and retracting northward in summer (Machalett et al., 2008), most likely increased the frequency and strength of cyclonic storms, leading to dust transport and the accumulation of loess deposits during cold phases when it predominated in the Ili Basin and along the Kyrgyz Tian Shan piedmont. Reviewer's note: I (this reviewer) failed to see the linkage between "southward-moving high-latitude air masses" and "migrated rain belt". I also failed to see the linkage between "enhanced evaporation" and "strengthened westerly winds". Consequently, I failed to see the logic of your reasoning: the Arctic polar front, intruding southward in the winter and retracting northward in summer (Machalett et al., 2008), most likely increased the frequency and strength of cyclonic storms during cold phases. At least, you have to say more about the logic of your reasoning.

A&R: In this respect our logic was flawed. We have clarified the logic of our arguments in the text. As mentioned above, it is unreasonable to draw conclusions beyond the information available in the data. Therefore, we reconsidered the atmospheric system responsible for aeolian dust dynamics in our study area, and then rewrote and rearranged the paragraphs.

As explained above, the Siberian high-pressure systems exerted a significant influence on wind dynamics responsible for dust transport and the accumulation of loess deposits during cold phases in NLK, and the mid-latitude Westerlies controlled the patterns of moisture variations in Arid Central Asia (ACA), based on modern and Holocene climate data and comparison of the EM1 proportions and mean grain size (MGS) data from the Jingyuan section in northwestern CLP. A strengthened Siberian High would push the mid-latitude Westerlies pathways further to the south, which resulted in comparably drier conditions in the northern Central Asia regions (e.g. Tianshan Mountains) but wetter conditions in south-western Central Asia (Pamir) (Lei et al., 2014; Wolff et al., 2017). Intensity and geographical position of the Siberian High can strongly control precipitation and atmospheric circulation patterns (meridional or zonal) at mid-latitudes of Asia (Panagiotopoulos et al., 2005). Therefore, the coupling of the Siberian High with the mid-latitude Westerlies system likely contributed significantly to the climate variability in the study area, which may interpret the seesaw relationship during MIS3 shown in Fig. 7 of manuscript.

Replies to the comments of editor

C&S: Please revise your manuscript by incorporating the changes that you have made in response

to the referees' comments. My concern with this manuscript is that the discussions and conclusions are based on one loess section. The title with the words such as environmental dynamics doesn't really reflect the level of science that you try to convey in the manuscript. Please re-consider the title.

A&R: We have rechecked and further considered the correlation of EM1 proportions and GISP $\delta^{18}\text{O}$ from the Greenland ice cores. Although it may not be possible to reliably match fluctuations in loess records to millennial climatic events due to the limitations in dating techniques in loess research, our grain-size proxy data can still correlate with abrupt events, such as Heinrich events (H1 to H6) identified from the North Atlantic records (Fig. 7 in the revised manuscript). However, EM1 proportions fluctuate weaker in H2 and H5 events, which we attribute to availabilities of source sediments, as mentioned above. These millennial-scale events were also found in Xiaoerbulake section, Taleda section and Zhaosu section from the Ili Basin (Li et al., 2016a; Li et al., 2011a; Zhang et al., 2015). However, in our opinion, the Siberian high-pressure systems predominate in the Ili Basin during cold phases, which leads to dust transport and increased loess accumulation at NLK and is responsible for those North Atlantic millennial scale abrupt climate events. Therefore, our data support the Siberian High can also transport the climatic signals in the North Atlantic to the East Asia, via the ice sheets in high northern latitudes. Moreover, lack of good correlation between EM1 proportions and GISP $\delta^{18}\text{O}$ values during relatively mild interstadial periods (Dansgaard-Oeschger cycles) when the mid-latitude westerlies shift northwards, implies the minor direct influences of the mid-latitude westerlies on the loess accumulation in NLK, which is not in agreement with the previous studies.

In addition, some of the peaks in EM1 curve correspond to valleys in GISP $\delta^{18}\text{O}$ curve (black arrows in Fig. 7 in the manuscript) except Heinrich events, yet many do not (pink dashed lines in Fig. 7 in the manuscript). The same case also occurs in the Western CLP (Chen et al., 1997), that is, all of the Heinrich events occurred during periods of strong winter monsoon in China, but not all of the periods of strong winter monsoon in China correlate with Heinrich events in the North Atlantic. The differences may be because the loess records in our study area represent a response not only to global signals but also local signals such as local atmospheric circulation and topography.

We have rewritten the title, "Aeolian dust dispersal patterns since the last glacial period in eastern Central Asia: Insights from a loess-paleosol sequence in the Ili Basin, northwest China". Thank you.

References

- Cai, Y. J., Chiang, J. C. H., Breitenbach, S. F. M., Tan, L. C., Cheng, H., Edwards, R. L., and An, Z. S.: Holocene moisture changes in western China, Central Asia, inferred from stalagmites, *Quaternary Sci Rev*, 158, 15-28, 2017.
- Chen, F., Bloemendal, J., Wang, J., Li, J., and Oldfield, F.: High-resolution multi-proxy climate records from Chinese loess: evidence for rapid climatic changes over the last 75 kyr, *Palaeogeography, Palaeoclimatology, Palaeoecology*, 130, 323-335, 1997.
- Chen, X., Song, Y., Li, J., Fang, H., Li, Z., Liu, X., Li, Y., and Orozbaevd, R.: Size-differentiated REE characteristics and environmental significance of aeolian sediments in the Ili Basin of Xinjiang, NW China, *Journal of Asian Earth Sciences*, 143, 30-38, 2017.
- Cheng, H., Zhang, P. Z., Spotl, C., Edwards, R. L., Cai, Y. J., Zhang, D. Z., Sang, W. C., Tan, M.,

and An, Z. S.: The climatic cyclicity in semiarid-arid central Asia over the past 500,000 years, *Geophysical Research Letters*, 39, Artn L01705
10.1029/2011gl050202, 2012.

Derbyshire, E., Meng, X. M., and Kemp, R. A.: Provenance, transport and characteristics of modern aeolian dust in western Gansu Province, China, and interpretation of the Quaternary loess record, *Journal of Arid Environments*, 39, 497-516, DOI 10.1006/jare.1997.0369, 1998.

Ding, Z., Liu, T., Rutter, N. W., Yu, Z., Guo, Z., and Zhu, R.: Ice-volume forcing of East Asian winter monsoon variations in the past 800,000 years, *Quaternary Res*, 44, 149-159, 1995.

Falkovich, A. H., Ganor, E., Levin, Z., Formenti, P., and Rudich, Y.: Chemical and mineralogical analysis of individual mineral dust particles, *Journal of Geophysical Research: Atmospheres*, 106, 18029-18036, 2001.

Gaiero, D. M., Simonella, L., Gassó, S., Gili, S., Stein, A. F., Sosa, P., R. Becchio, Arce, J., and Marelli, H.: Ground/satellite observations and atmospheric modeling of dust storms originating in the high Puna-Altiplano deserts (South America): Implications for the interpretation of paleo-climatic archives, *Journal of Geophysical Research: Atmospheres*, 118, 3817-3831, 2013.

Gong, D. Y., and Ho, C. H.: The Siberian High and climate change over middle to high latitude Asia, *Theor Appl Climatol*, 72, 1-9, 2002.

Hamzeh, M. A., Gharaie, M. H. M., Lahijani, H. A. K., Djamali, M., Harami, R. M., and Beni, A. N.: Holocene hydrological changes in SE Iran, a key region between Indian Summer Monsoon and Mediterranean winter precipitation zones, as revealed from a lacustrine sequence from Lake Hamoun, *Quaternary International*, 408, 25-39, 2015.

Hao, Q., Wang, L., Oldfield, F., Peng, S., Qin, L., Song, Y., Xu, B., Qiao, Y., Bloemendal, J., and Guo, Z.: Delayed build-up of Arctic ice sheets during 400,000-year minima in insolation variability, *Nature*, 490, 393-396, 2012.

Huang, W., Chen, J. H., Zhang, X. J., Feng, S., and Chen, F. H.: Definition of the core zone of the "westerlies-dominated climatic regime", and its controlling factors during the instrumental period, *Science China-Earth Sciences*, 58, 676-684, 10.1007/s11430-015-5057-y, 2015.

Huang, X. T., Oberhansli, H., von Suchodoletz, H., and Sorrel, P.: Dust deposition in the Aral Sea: implications for changes in atmospheric circulation in central Asia during the past 2000 years, *Quaternary Sci Rev*, 30, 3661-3674, 2011.

Lei, Y. B., Tian, L. D., Bird, B. W., Hou, J. Z., Ding, L., Oimahmadov, I., and Gadoev, M.: A 2540-year record of moisture variations derived from lacustrine sediment (Sasikul Lake) on the Pamir Plateau, *Holocene*, 24, 761-770, 2014.

Li, C., Song, Y., Qian, L., and Wang, L.: History of climate change recorded by grain size at the Zhaosu loess section in the Central Asia since the last glacial period, *Acta Sedimentologica Sinica*, 29, 1170-1179 (in Chinese with English abstract), 2011a.

Li, X., Zhao, K., Dodson, J., and Zhou, X.: Moisture dynamics in central Asia for the last 15 kyr: new evidence from Yili Valley, Xinjiang, NW China, *Quaternary Sci Rev*, 30, 3457-3466, 2011b.

Li, Y., Song, Y., Lai, Z., Han, L., and An, Z.: Rapid and cyclic dust accumulation during MIS 2 in Central Asia inferred from loess OSL dating and grain-size analysis, *Scientific Reports*, 6, DOI: 10.1038/srep32365, 2016a.

Li, Y., Song, Y. G., Lai, Z. P., Han, L., and An, Z. S.: Rapid and cyclic dust accumulation during MIS 2 in Central Asia inferred from loess OSL dating and grain-size analysis, *Scientific Reports*, 6, 2016b.

- Lin, Y. C., Mu, G. J., Xu, L. S., and Zhao, X.: The origin of bimodal grain-size distribution for aeolian deposits, *Aeolian Res*, 20, 80-88, 10.1016/j.aeolia.2015.12.001, 2016.
- Liu, X., Liu, T., Paul, H., Xia, D., Jiri, C., and Wang, G.: Two pedogenic models for paleoclimatic records of magnetic susceptibility from Chinese and Siberian loess, *Science in China Series D: Earth Sciences*, 51, 284-293, 2008.
- Liu, X. M., Hesse, P., Rolph, T., and Begét, J. E.: Properties of magnetic mineralogy of Alaskan loess: evidence for pedogenesis, *Quatern Int*, 62, 93-102, 1999.
- Machalett, B., Oches, E. A., Frechen, M., Zoller, L., Hambach, U., Mavlyanova, N. G., Markovic, S. B., and Endlicher, W.: Aeolian dust dynamics in central Asia during the Pleistocene: Driven by the long-term migration, seasonality, and permanency of the Asiatic polar front, *Geochemistry Geophysics Geosystems*, 9, Artn Q08q09 10.1029/2007gc001938, 2008.
- Mason, J. A., Greene, R. S., and Joeckel, R. M.: Laser diffraction analysis of the disintegration of aeolian sedimentary aggregates in water, *Catena*, 87, 107-118, 2011.
- Nottebaum, V., Stauch, G., Hartmann, K., Zhang, J. R., and Lehmkuhl, F.: Unmixed loess grain size populations along the northern Qilian Shan (China): Relationships between geomorphologic, sedimentologic and climatic controls, *Quatern Int*, 372, 151-166, 10.1016/j.quaint.2014.12.071, 2015.
- Panagiotopoulos, F., Shahgedanova, M., Hannachi, A., and Stephenson, D. B.: Observed trends and teleconnections of the Siberian high: A recently declining center of action, *J Climate*, 18, 1411-1422, 2005.
- Prins, M. A., and Vriend, M.: Glacial and interglacial eolian dust dispersal patterns across the Chinese Loess Plateau inferred from decomposed loess grain-size records, *Geochemistry Geophysics Geosystems*, 8, Artn Q07q05 10.1029/2006gc001563, 2007.
- Prins, M. A., Vriend, M., Nugteren, G., Vandenberghe, J., Lu, H. Y., Zheng, H. B., and Weltje, G. J.: Late Quaternary aeolian dust input variability on the Chinese Loess Plateau: inferences from unmixing of loess grain-size records, *Quaternary Sci Rev*, 26, 230-242, 10.1016/j.quascirev.2006.07.002, 2007.
- Pye, K.: *Aeolian Dust and Dust Deposits*, in, Academic Press, London, 29-62, 1987.
- Pye, K.: The nature, origin and accumulation of loess, *Quaternary Sci Rev*, 14, 653-667, Doi 10.1016/0277-3791(95)00047-X, 1995.
- Qiang, M., Lang, L., and Wang, Z.: Do fine-grained components of loess indicate westerlies: Insights from observations of dust storm deposits at Lenghu (Qaidam Basin, China), *Journal of Arid Environments*, 74, 1232-1239, 10.1016/j.jaridenv.2010.06.002, 2010.
- Ramisch, A., Lockot, G., Haberzettl, T., Hartmann, K., Kuhn, G., Lehmkuhl, F., Schimpf, S., Schulte, P., Stauch, G., Wang, R., Wünnemann, B., DadaYan, Zhang, Y., and Diekmann, B.: A persistent northern boundary of Indian Summer Monsoon precipitation over Central Asia during the Holocene, *Scientific reports*, 6, 2016.
- Rasmussen, S. O., Bigler, M., Blockley, S. P., Blunier, T., Buchardt, S. L., Clausen, H. B., Cvijanovic, I., Dahl-Jensen, D., Johnsen, S. J., Fischer, H., Gkinis, V., Guillevic, M., Hoek, W. Z., Lowe, J. J., Pedro, J. B., Popp, T., Seierstad, I. K., Steffensen, J. P., Svensson, A. M., Vallelonga, P., Vinther, B. M., Walker, M. J. C., Wheatley, J. J., and Winstrup, M.: A stratigraphic framework for abrupt climatic changes during the Last Glacial period based on three synchronized Greenland ice-core

records: refining and extending the INTIMATE event stratigraphy, *Quaternary Sci Rev*, 106, 14-28, 10.1016/j.quascirev.2014.09.007, 2014.

Sahsamanoglou, H. S., Makrogiannis, T. J., and Kallimopoulos, P. P.: Some Aspects of the Basic Characteristics of the Siberian Anticyclone, *Int J Climatol*, 11, 827-839, 1991.

Savelieva, N. I., Semiletov, I. P., Vasilevskaya, L. N., and Pugach, S. P.: A climate shift in seasonal values of meteorological and hydrological parameters for Northeastern Asia, *Prog Oceanogr*, 47, 279-297, 2000.

Sun, D., Su, R., Li, Z., and Lu, H.: The ultrafine component in Chinese loess and its variation over the past 7· 6 Ma: implications for the history of pedogenesis, *Sedimentology*, 58, 916-935, 2011.

Sun, D. H., Chen, F. H., Bloemendal, J., and Su, R. X.: Seasonal variability of modern dust over the Loess Plateau of China, *Journal of Geophysical Research-Atmospheres*, 108, Artn 4665 10.1029/2003jd003382, 2003.

Sun, Y. B., Wang, X. L., Liu, Q. S., and Clemens, S. C.: Impacts of post-depositional processes on rapid monsoon signals recorded by the last glacial loess deposits of northern China, *Earth and Planetary Science Letters*, 289, 171-179, 2010.

Ujvari, G., Kok, J. F., Varga, G., and Kovacs, J.: The physics of wind-blown loess: Implications for grain size proxy interpretations in Quaternary paleoclimate studies, *Earth-Science Reviews*, 154, 247-278, 10.1016/j.earscirev.2016.01.006, 2016.

Vandenberghe, J., Renssen, H., van Huissteden, K., Nugteren, G., Konert, M., Lu, H. Y., Dodonov, A., and Buylaert, J. P.: Penetration of Atlantic westerly winds into Central and East Asia, *Quaternary Sci Rev*, 25, 2380-2389, 10.1016/j.quascirev.2006.02.017, 2006.

Vandenberghe, J.: Grain size of fine-grained windblown sediment: A powerful proxy for process identification, *Earth-Science Reviews*, 121, 18-30, 2013.

Vandergoes, M. J., Newnham, R. M., Preusser, F., Hendy, C. H., Lowell, T. V., Fitzsimons, S. J., Hogg, A. G., Kasper, H. U., and Schlüchter, C.: Regional insolation forcing of late Quaternary climate change in the Southern Hemisphere, *Nature*, 436, 242-245, 2005.

Vriend, M., Prins, M. A., Buylaert, J. P., Vandenberghe, J., and Lu, H. Y.: Contrasting dust supply patterns across the north-western Chinese Loess Plateau during the last glacial-interglacial cycle, *Quatern Int*, 240, 167-180, 10.1016/j.quaint.2010.11.009, 2011.

Wang, X., Lang, L., Hua, T., Zhang, C., and Li, H.: The effects of sorting by aeolian processes on the geochemical characteristics of surface materials: a wind tunnel experiment, *Frontiers of Earth Science*, 1-9, 2017.

Wolff, C., Plessen, B., Dudashvili, A. S., Breitenbach, S. F., Cheng, H., Edwards, L. R., and Strecker, M. R.: Precipitation evolution of Central Asia during the last 5000 years, *Holocene*, 27, 142-154, 2017.

Yang, F., Zhang, G. L., Yang, F., and Yang, R. M.: Pedogenetic interpretations of particle-size distribution curves for an alpine environment, *Geoderma*, 282, 9-15, 2016.

Ye, W., Sang, C., and Zhao, X.: Spatial-temporal distribution of loess and source of dust in Xinjiang, *Journal of Desert Research*, 23, 514-520 (in Chinese), 2003.

Zhang, W., Shi, Z., Liu, Y., Su, H., and Niu, J.: Climatic record in the loess-paleosol sediment in the Ili basin and comparative analysis with the Heinrich events, *Journal of Geology and Geocryology*, 37, 973-979 (in Chinese with English abstract), 2015.

Zhang, X. Y., Arimoto, R., and An, Z. S.: Glacial and interglacial patterns for Asian dust transport, *Quaternary Sci Rev*, 18, 811-819, 1999.

A list of all relevant changes made in the manuscript

Line numbers in following parts refer to those in the *Marked-up Manuscript*.

Figure

1. We have improved the quality of Figure 1, changed front size and enlarged this figure.
2. We added the mean grain size record of the Jingyuan loess section and U-ratios (15.6–63.4 μm /5.61–15.6 μm) of the SE Kazakhstan loess to Figure 7, in an effort to support our argument that the Siberian high-pressure system exerts a significant influence on wind dynamics and therefore loess deposition processes at NLK.

Running text

1. Line 1-4: We have rewritten the title.
2. Line 27: We substituted “records” with “archives”.
3. Line 29-37: We have simplified and clarified our expression regarding MS.
4. Line 39-40: “are inferred to” was added into this sentence and “the” was deleted.
5. Line 41-42: We substituted “the” with “a”, and “processes” with “conditions”.
6. Line 43-60: We have rewritten this part according to the revised section 5.3 to make the abstract more logical, and have clarified that the Siberian high-pressure system was most likely the strongest influence on wind dynamics and thus the loess deposition in NLK.
7. Line 67-69: The range of arid Central Asia is defined.
8. Line 75-76: We substituted “Central Asian region” with “ACA”.
9. Line 77-78: We deleted the repetitive sentence.
10. Line 79-82: We added names of the mountain ranges where Central Asia piedmont loess is distributed.
11. Line 85-87: We have simplified our expression.
12. Line 89: We substituted “temperature” with “millennial-scale climatic”.
13. Line 92-100: We have simplified our expression.
14. Line 101-110: We have simplified and clarified our expression and the objective of this paper.
15. Line 113-117: We have simplified these sentences.
16. Line 125-126: We added the modern meteorological data on MAP and MAT at NLK.
17. Line 127-129 and 135-137: We changed the position of this sentence.
18. Line 146: We deleted the sentence “confirmed by our subsequent grain size and magnetic susceptibility (MS) results”.
19. Line 149-155: We have simplified and clarified these sentences.
20. Line 165: We have deleted “established by”, and rewritten the words, like this “(BEMMA; Yu et al. (2016))”.
21. Line 168-172: We have clarified the measurement processes of quartz grain size.
22. Line 177: We added the word “precisely”.
23. Line 219 and 232: We have changed the position of Figure 4.
24. Line 236-237: We have changed the subtitle.
25. Line 238-265: We have simplified these two paragraphs and cut out everything that’s not necessary to make our meanings clearer.

26. Line 266-286: We have polished the language of these three paragraphs.
27. Line 291-293: We have substituted “typically conducive to” with “associated with”, and deleted “including high precipitation and rising groundwater levels”.
28. Line 297: We deleted the sentence “and yet very weak pedogenesis was reflected by χ_{fd} ”.
29. Line 300-301: We have deleted the first sentence of this paragraph.
30. Line 308-322: We have rewritten this paragraph and added a literature in order to state that the “wind theory” can be used to decipher the MS variations of NLK loess.
31. Line 324-357: We have added a comprehensive and streamlined review on existing literature dealing with interpretation of loess particle size, including the two dominant approaches to unmixing grain size spectra and successful applications of sediment groups according to Vandenberghe (2013) to interpret the multiple sources for loess sediments.
32. Line 368: We substituted “stocks” with “supplies”.
33. Line 370: We wrote “aeolian transport” to “entrainment”.
34. Line 381: We substituted “therefore” with “rather”.
35. Line 383: We clarified this sentence.
36. Line 388-390: We split original sentence into two sentences.
37. Line 195: “fallout” was added.
38. Line 401-402: We split original sentence into two sentences.
39. Line 413: We have clarified the statement of Zhang et al. (1999)
40. Line 423-425: We added a line of evidence for supporting that finer single particles could settle down during low velocity wind condition.
41. Line 427-440: We have simplified and clarified these sentences.
42. Line 467-474: We have clarified these sentences.
43. Line 489-493: We have revised the caption of Figure 7, and added two curves (MGS and U-ratio) and deleted the summer insolation curve.
44. Line 497: We have deleted the sentence “Based on the independent chronology sequences”.
45. Line 500-504: We have added two curves (MGS and U-ratio) and deleted the summer insolation curve.
46. Line 505-520: We clarified this paragraph.
47. Line 524-690: We have reconsidered and rewritten this part. We now list the arguments for the significant influence of the Siberian high-pressure system on wind dynamics and thus loess deposition in the eastern Ili Basin, and acknowledge the role of the mid-latitude Westerlies in controlling broad-scale patterns of moisture variation across ACA. The coupling of the Siberian High with the mid-latitude Westerlies system most likely had the strongest influence on climate variability at NLK in the eastern Ili Basin. Moreover, our data support the hypothesis that the Siberian High forms a teleconnection between the climatic systems of the North Atlantic and East Asia, via the ice sheets in high northern latitudes, with the exception of the mid-latitude westerlies. We have made the section 5.3 clearer and more logical.
48. Line 692-697: We have simplified and clarified our expression about MS.
49. Line 698: We have deleted the sentence “With the unmixing of grain size distributions”.
50. Line 706-720: We have revised the last part of conclusion according to the revised section 5.3.

1 ~~Environmental dynamics~~Aeolian dust patterns since the last glacial period
2 in ~~arid eastern~~ Central Asia: ~~evidence~~Insights from ~~grain size distribution~~
3 ~~and magnetic properties of a loess-paleosol sequence from the Ili Valley in~~
4 the Ili Basin, western China

5 Yue Li^{1,2}, Yougui Song^{1*}, Kathryn E. Fitzsimmons³, Hong Chang¹, Rustam Orozbaev^{4,5}, Xinxin Li
6 ^{1,2}

7 1 State Key Laboratory of Loess and Quaternary Geology, Institute of Earth Environment, Chinese
8 Academy of Sciences, Xi'an, 710061, China

9 2 College of Earth Science, University of Chinese Academy of Sciences, Beijing, 100049, China

10 3 Research Group for Terrestrial Palaeoclimates, Max Planck Institute for Chemistry, Hahn-
11 Meitner-Weg 1, 55128 Mainz, Germany

12 4 Research Center for Ecology and Environment of Central Asia, Chinese Academy of Sciences,
13 Urumqi, 830011, China

14 5 Institute of Geology, National Academy of Sciences, Bishkek, 720040, Kyrgyzstan

15

16 * Corresponding author:

17 Dr. Yougui Song

18 E-mail: syg@ieecas.cn

19 State Key Laboratory of Loess and Quaternary Geology

20 Institute of Earth Environment, Chinese Academy of Sciences

21 No. 97 Yanxiang Road, Yanta, Xi'an 710061, China

22 Tel. 86-29 6233 6216

23 Fax. 86-29 6233 6216

24

25 Abstract

26 The extensive loess deposits of the Eurasian mid-latitudes provide important terrestrial
27 ~~archives records~~ of Quaternary climatic change. As yet, however, loess records in Central Asia are
28 poorly understood. Here we investigate the grain size and magnetic characteristics of loess from the
29 Nilka (NLK) section in the Ili Basin of eastern Central Asia. ~~Magnetic parameters indicate very~~
30 ~~weak pedogenesis compared with loess from other regions in Eurasia. Weak pedogenesis suggested~~
31 ~~by frequency-dependent magnetic susceptibility (χ_{fd} %) and magnetic susceptibility (MS) peaks~~ The
32 ~~higher χ_{fd} values occur~~ in primary loess ~~suggest that MS is more strongly influenced by allogenic~~
33 ~~magnetic minerals than pedogenesis, and may therefore be used to indicate wind strength. This is~~
34 ~~supported by the close correlation between variations in MS and proportions of the sand-sized~~
35 ~~fraction, rather than in weak paleosols, and the variations in magnetic susceptibility (MS) value~~
36 ~~correlate closely with the proportions of the sand fraction. We attribute this result to high wind~~
37 ~~strength at the time of loess deposition.~~ To further explore the ~~temporal variability in~~ dust transport
38 patterns ~~further~~, we identified three grain size end members (EM1, mode size 47.5 μm ; EM2, 33.6
39 μm ; EM3, 18.9 μm) which represent distinct aerodynamic environments. EM1 and EM2 ~~are inferred~~
40 ~~to represent the~~ grain-size fractions transported from proximal sources in short-term, near-surface
41 suspension during dust outbreaks. EM3 appears to represent ~~the a~~ continuous background dust
42 fraction under non-dust storm ~~processes conditions~~. Of the three end members, EM1 is most likely
43 the most sensitive recorder of wind strength. ~~We compare our EM1 proportions and mean grain size~~
44 ~~from NLK with the Jingyuan section in the Chinese loess plateau, and assess these in the context of~~
45 ~~modern and Holocene climate data, and suggest that the Siberian high-pressure system is the~~
46 ~~dominant influence on wind dynamics and thus loess deposition in the eastern Ili Basin. Six~~
47 ~~millennial-scale cooling (Heinrich) events can be identified in the NLK loess records. Our grain-~~
48 ~~size data support the hypothesis that the Siberian High acts as teleconnection between the climatic~~
49 ~~systems of the North Atlantic and East Asia in the high northern latitudes, but not for the mid-~~
50 ~~latitude westerlies. A lack of correlation between EM1 proportions and GISP $\delta^{18}\text{O}$ values at the~~
51 ~~millennial scale, combined with modern weather data, suggests that Arctic polar front predominates~~
52 ~~in the Ili Basin and the Kyrgyz Tian Shan piedmont during cold phases, which leads to the dust~~
53 ~~transport and accumulation of loess deposits, while the shift of mid-latitude westerlies towards the~~
54 ~~south and north controls the patterns of precipitation/moisture variations in this region. Comparison~~
55 ~~of EM1 proportions with Northern Hemisphere summer insolation clearly illustrate local insolation-~~
56 ~~based control on wind dynamics in the region, and humidity can also influence grain size of loess~~
57 ~~over MIS3 in particular. Although, the polar front dominated wind dynamics for loess deposition in~~
58 ~~the region, the Central Asian high mountains obstructed its migration further south. Our results may~~
59 ~~also support the significance of the mid-latitude westerlies in transmitting North Atlantic climate~~
60 ~~signals to East Asia.~~

61
62 Key words: Last glacial, Ili Basin, Central Asia, loess, magnetic susceptibility, grain size,
63 paleoclimate

64 1 Introduction

65
66 Central Eurasia experiences extremely continental climatic conditions in large part due to its
67 position far from ~~the~~ oceans. Arid Central Asia (~~ACA~~), ~~the mid-latitude region spanning the Caspian~~
68 ~~Sea across to the eastern Tien Shan mountains~~, is therefore a sensitive recorder of past climate

带格式的：缩进：首行缩进： 0 字符

69 change due to its location in the transitional al region-zone between the Asian monsoon (Dettman et
70 al., 2001; Cheng et al., 2012), mid-latitude westerlies (Vandenberghe et al., 2006) and North Asian
71 polar front (Machalett et al., 2008). The relative influence and intensity of these major climate
72 subsystems have varied across the latitudinal and longitudinal range of Central Asia through time.
73 Thus identification of the predominant climate regimes in a certain region is a crucial precondition
74 for tracing paleoclimatic evolution.

75 One of the most promising potential palaeoenvironmental archives in the Central-Asian ACA
76 region is its widespread, thick loess deposits. Loess is one of the most important archives of
77 Quaternary climate change (Maher, 2016; Muhs, 2013). The semi-arid zone of Eurasia, between 45°
78 and 30° N, hosts some of the thickest and most extensive loess deposits in the world. In Central
79 Asia, the loess deposits cover drape the piedmont slopes of the major mountains ranges - the Tian
80 Shan mountains, Alai, Altai and Pamirs - from Xinjiang province of China and through Kazakhstan,
81 to Kyrgyzstan and Uzbekistan, into Tajikistan. While loess in Central Asia has increasingly formed
82 the focus of recent years have witnessed increasing loess-based datasets research in the region
83 (Dodonov et al., 2006; Feng et al., 2011; Li et al., 2016c; Li et al., 2016b; Machalett et al.,
84 2006; Smalley et al., 2006; Song et al., 2014; Song et al., 2015; Song et al., 2012; Yang et al.,
85 2006; Youn et al., 2014; Fitzsimmons et al., 2016), as yet the forcing mechanisms and the climatic
86 conditions responsible for loess-paleosol sequences formation are as yet ambiguous, and the
87 paleoclimatic evolution recorded by these loess deposits in this region is not systematically
88 understood (Li et al., 2016a; Fitzsimmons et al., 2016; Machalett et al., 2008).

89 Evidence for temperature-millennial-scale climatic oscillations associated with the Greenland
90 (*Dansgaard/Oeschger (D-O) events*) (Dansgaard et al., 1993) and cool phases associated with
91 iceberg calving into the North Atlantic (*Heinrich (H) events*) (Bond et al., 1992) have been found
92 in the form of loess deposits based on the high-resolution grain-size variations ether in loess deposits
93 in Chinese Loess Plateau (CLP) loess (Sun et al., 2012; Porter and An, 1995; Chen et al., 1997b) or
94 in and European loess (Antoine et al., 2009; Rousseau et al., 2007; Zeeden et al., 2016). Climatic
95 teleconnections, especially between the North Atlantic and East Asian Monsoon regions, are likely
96 to have been recorded within the Data for Central Asian loess do not as yet exist. As yet, however,
97 the region so far largely lacks at this resolution, despite its strategic location as a likely
98 environmental bridge between the North Atlantic and East Asian Monsoon climatic regions, data by
99 which the role and contribution of the central parts of the Eurasian continent, as an environmental
100 bridge, can be elucidated.

101 The Ili Basin of Central Asia represents a region of hosts thick loess deposits in the strategic
102 central eastern part of ACA (Song et al., 2014) with high potential for investigating
103 palaeoenvironmental change for the region. The situation of the basin, is surrounded to the south
104 and north by the Tian Shan mountain range, and widening to the west and drains into endorheic
105 Lake Balkhash (Fig. 1), and provides a conducive situation for loess accumulation. which has
106 resulted in the widespread and thick loess deposits in this basin. In this paper we present new data
107 on the physical properties of a 20.4 m thick loess deposit at Nilka (NLK) in the eastern Ili Basin, ,
108 focusing on We investigate variations in grain size distributions and magnetic properties in order
109 to investigate likely links with environmental dynamics the enhancement mechanisms of magnetic
110 susceptibility in NLK loess and elucidate environmental dynamics based on grain size data.

2 Physical geography

The Ili Basin (80° ~ 85° E and 42° 30' ~ 44° 30' N) straddles southeast Kazakhstan and northwest China. It is an intermontane basin opening westward towards [the Ili drains into Lake Balkhash](#) ~~the semi-arid Kazakhstan Gobi Desert~~ which ~~forms is in the semi-arid the~~ transitional region between the steppe and full deserts of Central Asia. The Northern and Southern Tian Shan form the northern and southern ~~boundaries to margins of~~ the basin (Fig. 1a). ~~The Ili River drains northwestward into terminal Lake Balkhash.~~

This region has a semi-arid, continental climate, with a strong precipitation gradient dependent on altitude. The altitude of the basin floor is 500 ~ 780 m; the northern ~~Tien-Tian~~ Shan Range reaches altitudes of > 4000 m a.s.l. and the southern ~~Tien-Tian~~ Shan mountains range between 3000 ~ 7000 m a.s.l. towards the catchment divide. ~~The m~~ Mean annual precipitation (MAP) ranges between 200 ~~mm and~~ 500 mm on the plains, and mean annual temperature (MAT) ranges from 2.6°C ~~to~~ 10.4°C (Li, 1991; Ye, 1999). The surface vegetation in this region is dominated by *Desert Steppe* and *Steppe* and the zonal soils comprise *Sierozem*, *Castanozem* and *Chernozem*.

[Modern meteorological data \(2009 – 2013\) show a MAP of 354 mm and a MAT of 7.3°C in Nilka site \(data from the China Meteorological Data Network: <http://data.cma.cn/>\).](#)

~~The Nilka (NLK) section (83.25°E, 43.76°N, 1253 m a.s.l) is situated on the second terrace of the right bank of the Kashi River, a tributary of the Ili River. The site is located in the eastern Ili Basin of far western China, adjoining the Northern Tian Shan to the north (Fig. 1b).~~

Fig. 1 The location of study area and the photo of Nilka (NLK) section.

3 Materials and methods

3.1 Section and sampling

[The Nilka \(NLK\) section \(83.25°E, 43.76°N, 1253 m a.s.l\) is situated on the second terrace of the right bank of the Kashi River, a tributary of the Ili River. The site is located in the eastern Ili Basin of far western China, adjoining the Northern Tian Shan to the north \(Fig. 1b\).](#)

~~The NLK loess~~ section has a thickness of 20.4 m and overlies fluvial sands and gravels (Fig. 1c). The profile has been exposed recently by local residents for making bricks, and recently formed the focus of a geochronological study comparing luminescence with radiocarbon methods (Song et al., 2015). According to the dating results ~~of~~, the NLK loess started to accumulate since ~ 70 ka ~~B.P.~~. Stratigraphically and geochronologically, this is equivalent to the L1 loess unit (known as Malan loess) and S0 paleosol unit (also known as Holocene Heilu soil) in the ~~Chinese Loess Plateau CLP~~ (Liu, 1985a), ~~2300 km to the east~~. Although largely homogeneous in appearance, two weak paleosols (at 5.04 – 7 m and 15.7 – 18 m depths) were identified in the section by field observations ~~and confirmed by our subsequent grain-size and magnetic susceptibility (MS) results.~~ We therefore divided the NLK stratigraphy into S0, L1L1, L1S1, L1L2, L1S2 and L1L3 units (Fig. 1c).

~~Following After~~ cleaning ~~back of~~ the NLK section to remove dry, weathered sediment, samples were collected at intervals of 2 cm. A total of 1026 bulk samples were prepared for measurements of physical characteristics. [Because the optically stimulated luminescence \(OSL\) dating is more reliable for constructing a loess chronology than bulk sediment AMS ¹⁴C dates \(Song et al., 2015\).](#) ~~This study uses the previously published more reliable optically stimulated luminescence (OSL) dating results as basis for the our age model and assessment of the evolution of loess physical~~

characteristics.

3.2 Grain-size analyses

Prior to grain size measurements, 0.5 g of dry bulk sample was pretreated by removal of organic matter and carbonate using H_2O_2 and HCl, respectively (Lu and An, 1997). Samples were then dispersed for 5 min by ultrasonification with 10 ml 10% $(NaPO_3)_6$ solution. Grain size distribution was analysed using a Malvern 2000 laser instrument at the State Key Laboratory of Loess and Quaternary Geology, Institute of Earth Environment, Chinese Academy of Sciences. Particle size distribution was calculated for 100 grain size classes within a measuring range of 0.02–2000 μm . Replicate analyses indicated an analytical error of < 2% for the mean grain size.

End-member unmixing of loess grain-size distributions is based on the hierarchical Bayesian model for end-member modeling analysis (BEMMA) established by Yu et al. (2016). Grain-size parameters were calculated from the analytical data with GRADISTAT (Version 4.0; Blott (2000)).

2 samples (NLK1106 at 11.06 m and NLK1840 at 17.8 m) were also selected for the extraction and measurement of mineral-specific quartz grain sizes according to published methods of Sun et al. (2000a). The isolated quartz grain samples (Fig. S1) were then placed into analyzed by the Malvern 2000 laser instrument for mineral-specific grain size measurements so that comparisons of quartz grain and bulk samples could be performed to illustrate the weathering degree of NLK loess visually.

3.3 Magnetic susceptibility measurements

Magnetic susceptibility was measured with a Bartington MS2 meter at the State Key laboratory of Loess and Quaternary Geology, Institute of Earth Environment, Chinese Academy of Sciences. Samples were oven-dried at 40°C for 24 hours. Subsamples of 10 g from each sample were then precisely weighed for magnetic measurements. Low- (0.47 kHz) and high- (4.7 kHz) frequency magnetic susceptibility (χ_{lf} and χ_{hf} , respectively) were measured. The absolute frequency-dependent magnetic susceptibility was calculated as $\chi_{fd} = \chi_{lf} - \chi_{hf}$. Frequency-dependent magnetic susceptibility was defined and calculated as $\chi_{fd} \% = [(\chi_{lf} - \chi_{hf}) / \chi_{lf}] \times 100\%$.

4 Results

4.1 Magnetic susceptibility variations

Both magnetic susceptibility (MS) data and stratigraphy show a close correspondence throughout the NLK section. We observe higher MS values within primary loess and lower values within paleosols. The exception to this trend is the modern (S0) soil in which yields high MS values are presented (Fig. 2).

Fig. 2 Lithology and magnetic susceptibility characteristics (χ_{lf} , χ_{fd} and $\chi_{fd}\%$) of the NLK section.

The low-frequency magnetic susceptibility (χ_{lf}) values of the S0 unit are higher than for the L1 unit, with an average of $98.13 \times 10^{-8} m^3 kg^{-1}$. The χ_{lf} values of the L1L1 unit vary from $56.5 - 103.9 \times 10^{-8} m^3 kg^{-1}$, with a decreasing trend down-profile. The χ_{lf} value abruptly decreases at c. 5 m, with generally lower values in the L1S1 unit, averaging $62.58 \times 10^{-8} m^3 kg^{-1}$. χ_{lf} in the L1L2 unit gradually increases down profile, with significant fluctuations in the lower part; χ_{lf} values vary from $67 - 102.55 \times 10^{-8} m^3 kg^{-1}$. Lower χ_{lf} values are observed in L1S1 unit with an average value of $57.99 \times 10^{-8} m^3 kg^{-1}$. In the L1L3 unit, the χ_{lf} values vary with greater amplitude around an average value of $68.74 \times 10^{-8} m^3 kg^{-1}$.

Absolute frequency-dependent magnetic susceptibility (χ_{fd}) values likewise vary with

199 stratigraphy. The S0 unit yields the highest χ_{fd} value. The L1 unit is characterized by relatively
200 consistent and lower χ_{fd} values. Frequency-dependent magnetic susceptibility ($\chi_{fd}\%$) yields the same
201 trend as χ_{fd} , although $\chi_{fd}\%$ values clearly increase in the central part of L1S2.

202 4.2 Mixing model of loess grain-size distributions

203 The mean grain-size distribution, and variation range of volume frequencies for each grain-
204 size class in the dataset, are presented in Fig. 3a. The overall grain-size frequency curve shows a
205 unimodal pattern, if slightly skewed towards the coarser side, with the primary mode ranging from
206 11.9 ~~μm~~ to 47.5 μm . An additional small grain size peak occurs at c. 0.4 – 2 μm . Three unmixed
207 end members were identified (Fig. S2), yielding fine-skewed grain-size distributions with clearly
208 defined modes of 47.5 μm (EM1), 33.6 μm (EM2) and 18.9 μm (EM3) (Fig. 3b).

209
210 Fig. 3 End-member modelling results of the grain-size dataset of the NLK section. (a) Mean size
211 distribution and range of volume frequency for each size class. (b) Modelled end-members
212 according to the three-end-member model (modal size: ~ 47.5 μm , ~ 33.6 μm and ~ 18.9 μm).
213 Size limits of clay, silt and sand fractions determined by laser particle sizer are differ from those
214 derived by the pipette method. The upper limits of grain-size classes used here are at 4.6/5.5 μm
215 for clay, 26 μm for fine silt, and 52 μm for coarse silt, as previously published by Konert and
216 Vandenberghe (1997). Sand is designated for particle sizes > 52 μm . Therefore, EM1 and EM2
217 correspond to coarse silt and EM3 to fine silt.

218
219 ~~Fig. 4 Proportional contributions of the three end-members in the NLK section.~~

220
221 The proportional distribution of the end members down the section is shown in Fig. 4. In the
222 primary loess units (L1L1, L1L2 and L1L3), the deposits are dominated by the coarser silt EM1 and
223 EM2, while higher proportions of fine silt EM3 are ~~preferentially~~ observed within the soil horizons
224 (S0, L1S1 and L1S2). EM1 displays high frequency, large amplitude fluctuations down the profile,
225 varying between 0.09 – 0.72, and clearly dominates the primary loess units and occurs in low
226 proportions in the soil units (Fig. 4). EM2 shows a similar trend to EM1, but with less variability
227 down profile. Proportions of EM2 range between 0.11 – 0.66 with minimal fluctuations within
228 individual units, and proportions decrease significantly in the soil units S0 and L1S2. Proportions
229 of EM3 remain consistently low within the primary loess units, and increase to 0.46 and 0.8 within
230 the soil horizons S0 and L1S2 respectively.

231
232 ~~Fig. 4 Proportional contributions of the three end-members in the NLK section.~~

235 5 Discussion

236 5.1 ~~Impacts of wind strength on magnetic susceptibility variations~~ Likely mechanisms for the 237 ~~enhancement of magnetic susceptibility in Ili Basin loess~~

238 Magnetic susceptibility (MS) in loess is ~~predominantly determined by~~ ~~due to~~ the concentration
239 of iron-bearing magnetic minerals within the sediment (Liu et al., 1999; Liu et al., 1994; Song et al.,
240 2010). ~~At the broadest level~~ Generally, this varies between primary loess, ~~and~~ ~~soil~~ horizons, with
241 soils generally ~~experiencing~~ ~~experience~~ an enrichment ~~of in~~ magnetic minerals (~~higher MS~~), ~~and~~
242 ~~corresponding higher MS values, than compared with~~ primary loess deposits (Zhou et al.,

带格式的: 缩进: 首行缩进: 2 字符

243 1990;Maher and Thompson, 1992;Heller and Evans, 1995;Heller and Liu, 1984;Ding et al.,
244 2002;Buggle et al., 2009). ~~The formation *in situ* of < 100 nm magnetite or maghemite grains during~~
245 ~~pedogenesis is the most widely accepted interpretation for the mechanisms of loess MS~~
246 ~~enhancement. Increased precipitation is conducive to chemical weathering and biological processes~~
247 ~~during pedogenesis. Song et al. (2010) further argued that strong pedogenesis under warm, humid~~
248 ~~climatic conditions produces new magnetic minerals.~~

249 The contrast between high and low MS in paleosols and primary loess, respectively, ~~has~~
250 ~~typically formed~~ the basis for the stratigraphic differentiation of loess deposits. ~~This principle has~~
251 ~~provided the foundation for large-scale correlations between loess deposits and with global~~
252 ~~climatic oscillations, initially in the Chinese Loess Plateau deposits and increasingly worldwide.~~

253 The main MS variations in the NLK loess sequence, with the exception of the S0 unit, however, do
254 not occur directly in association with pedogenesis (Fig. 2). ~~At NLK, lower MS values are found in~~
255 ~~the paleosols and higher MS in loess units.~~ A similar case also occurs in the L1 loess layers ~~at other~~
256 ~~sites in the Ili Valley, such as in the~~ TLD, ZKT and AXK sections, ~~also in the Ili valley~~ (Fig. 1) (Jia
257 et al., 2010;Jia et al., 2012;Song et al., 2010). ~~The lack of a straightforward correlation between MS,~~
258 ~~loess and paleosols indicates that an alternative explanation for this variability must be sought.~~
259 ~~Proposed mechanisms of variations in loess magnetic susceptibility include, in addition to~~
260 ~~pedogenesis, the dilution of relatively coarse silt with a low susceptibility, sediment compression~~
261 ~~and carbonate leaching, and decomposition of plant residues.~~

262 Since alternative mechanisms may have played a role in the magnetization of the Ili Basin loess
263 deposits, we investigated different aspects of environmental magnetic properties in order to
264 investigate to what degree pedogenesis or the alternative mechanisms played the more critical role
265 in this region.

266 Absolute frequency-dependent susceptibility (χ_{fd}) determines ~~indicates~~ the concentration of
267 magnetic particles within a small grain size range across the superparamagnetic (SP)/stable single
268 domain (SSD) boundary (Liu et al., 2012) (magnetite, <~100 nm; maghemite, <~20 μm). Particles
269 with this grain size are considered to form in situ within soils during pedogenesis (Maher and Taylor,
270 1988;Zhou et al., 1990), ~~and, therefore. Therefore,~~ χ_{fd} can serve as a direct proxy for pedogenesis
271 (Heller et al., 1993;Maher and Thompson, 1995;Liu et al., 2007;Buggle et al., 2014). In the NLK
272 section, χ_{fd} yields consistently low values throughout the sequence and indicates no clear ~~enrichment~~
273 ~~strong pedogenesis~~ even in the ~~weakly developed~~ paleosol layers (L1S1 and L1S2). Comparison
274 between χ_{lf} vs. χ_{fd} down profile shows no correlation between MS and SP particles (Fig. S3c). These
275 results suggest that SP particles played only a minor role in MS enhancement in the NLK loess.

276 Frequency-dependent magnetic susceptibility ($\chi_{fd}\%$) is used as a proxy to determine the
277 contribution of SP particles to MS (Zhou et al., 1990;Liu et al., 1992). At NLK ~~section,~~ however,
278 we ~~also~~ observe consistently low $\chi_{fd}\%$ values in both loess and paleosol layers, with a slight increase
279 only in the L1S1 paleosol. This observation reinforces our interpretation that the content of SP
280 particles is very low, and consequently that their contribution to MS can be ignored.

281 The low proportions of SP particles in the NLK loess imply that the pseudo-single-domain
282 (PSD) and multi-domain (MD) magnetic grains, rather than SP grains ~~forming in situ, are more~~
283 ~~influential for the make the more important contribution to~~ magnetic enhancement of NLK loess ~~at~~
284 ~~this site.~~ Since PSD and MD magnetic minerals are difficult to produce during pedogenesis (Song
285 et al., 2010), such minerals are more likely to be detrital in nature, deriving from the original
286 protolith.

带格式的: 缩进: 首行缩进: 0 字符, 制表位: 不在
6.08 字符

287
288
289
290
291
292
293
294
295
296
297
298
299
300
301
302
303
304
305
306
307
308
309
310
311
312
313
314
315
316
317
318
319
320
321
322
323
324
325
326
327
328
329
330

Fig. 5 Comparison of different grain size fractions of NLK loess with χ_{fd} (limits of grain-size classes after Konert and Vandenberghe (1997)).

In some cases, ~~the moist conditions typically conducive to~~ pedogenesis, including high precipitation and rising groundwater levels, may result in the weathering, ~~and destruction and~~ dissolution of the magnetic minerals maghemite and magnetite (Nawrocki et al., 1996; Maher, 1998; Grimley and Arruda, 2007). In such cases, a negative relationship between magnetic susceptibility and pedogenesis can develop, in contrast to the classical situation whereby χ_{fd} is enhanced. At NLK section, however, we observe no textures caused by groundwater fluctuations, ~~and yet very weak pedogenesis was reflected by χ_{fd} .~~ We therefore exclude groundwater fluctuations and high levels of precipitation as a factor in our MS characteristics at NLK section.

~~Increased concentrations of coarser grained detrital magnetic minerals, resulting from periods of increased wind strength, may enhance overall MS values.~~ In the wind velocity/vigor model (also known as the Alaskan or Siberian model), wind strength affects magnetic susceptibility values of loess through the physical sorting of magnetic grains (Beget and Hawkins, 1989). The influence of this process on MS values in loess can be assessed by investigating the correlation between MS and coarser (silt or sand) and finer clay percentages (Fig. S3). At NLK, low MS values in the S0 soil between 0 – 0.5 m correlate positively with clay percentage variations (Fig. S3a), while higher MS values at depths greater than > 0.5 m correlate closely with increased sand concentrations (Fig. S3b). We therefore propose that MS enhancement at NLK is primarily likely driven by wind strength, ~~increased concentrations of sand-sized detrital magnetic minerals, which increase during periods of stronger winds. The dilution effect of coarse particles with low susceptibility was excluded.~~ In the case of NLK, the reduced color contrast (Fig. 1) between loess and paleosol layers implies moderate climate fluctuations between loess deposition and pedogenesis due to generally more arid conditions than typically experienced in loess regions. Under this scenario, weak pedogenesis This prevented the efficient production of SP grains (Fig. 2), and allogenetic magnetic minerals associated with dust transportation made a greater contribution to the MS. Wind strength can therefore be interpreted regarded as a the main factor for influence on MS variations since last glacial At NLK. The enhancement of magnetic susceptibility in NLK loess most likely falls into region A in Fig. 9 of Liu et al. (2013). Region A represents the area where the climate is arid and pedogenesis is weak and, dominated by physical weathering (Liu et al., 2013). Therefore, we can use the “wind theory” to decipher the MS variations of NLK loess. Weak pedogenesis enables preservation of primary atmospheric dust contribution to NLK. And in turn, MS may be able to indicate stronger wind during dust storms.

5.2 Genetic interpretations of end members in loess grain size

~~In order to understand the atmospheric dynamic pattern during loess deposition further, we conducted unmixing of grain size distributions.~~

~~Recent years have seen increasing statistical analysis of loess grain size to identify subpopulations within bulk samples. From these statistical datasets, the different end members can be interpreted to infer distinct atmospheric transport mechanisms, modes and travel distances. In some cases, the end member approach has been used to identify variation in geological context, or source area. We investigated the utility of this approach to the Ili Basin loess at NLK by unmixing~~

带格式的：缩进：首行缩进： 0 字符

331 ~~grain-size distributions with BEMMA . As shown in Fig. S2, we generated a mixing model~~
332 ~~consisting of three end members.~~

333 Grain-size analysis was conducted in order to understand wind dynamics (strength and
334 direction) during loess deposition (Liu, 1985b;Lu and An, 1998;Sun et al., 2010). Grain-size
335 analysis provides information on sediment depositional mechanisms as well as an insight into
336 spatio-temporal changes in deposition, provided factors such as vegetation, pedogenesis, grain size
337 of source sediments, and distance from the deposition area to source area are taken into account
338 (Qin et al., 2005;DiPietro et al., 2017;Obreht et al., 2015;Terhorst et al., 2012;Ding et al., 2005;Ding
339 et al., 1999;Yang and Ding, 2008).

340 Statistical analysis of loess grain-size offers new opportunities for understanding paleoclimate
341 variations. Studies increasingly use grain size partitioning to identify subpopulations within bulk
342 samples. There are two dominant approaches to unmixing grain size spectra: parametric
343 decomposition (e.g. Sun et al., 2002) and non-parametric decomposition (e.g. Prins and Vriend,
344 2007;Weltje, 1997; Weltje and Prins, 2007) .Based on the statistical datasets generated, the different
345 end members can be interpreted to infer distinct atmospheric transport mechanisms, modes and
346 travel distances (Ujvari et al., 2016). In some cases, the end-member approach has been used to
347 identify variation in the geological context or source area (Prins et al., 2007). We investigated the
348 applicability of this approach to the Ili Basin loess at NLK by unmixing grain-size distributions with
349 BEMMA (Yu et al., 2016), generating a mixing model consisting of three end members (Fig. S2).

350 Relying largely on samples from Eurasian loess belt extending from the Russian Plain north of
351 the Caspian Sea eastwards to the Tibetan Plateau and CLP, Vandenberghe (2013) applied the visual
352 inspection of grain-size distribution curves and EMMA end-member analysis to define the
353 characteristic grain-size distribution of primary loess deposits and interpret the likely conditions of
354 transport and deposition. Using the sediment groups identified in Vandenberghe (2013), some
355 studies interpreted multiple sources for loess sediments (Yang et al., 2016;Nottebaum et al.,
356 2015;Nottebaum et al., 2014). In this study, we apply the end-member analysis of the NLK loess to
357 the sediment groups of Vandenberghe (2013) in an effort to reconstruct dominant aeolian processes.

358 Fine sand ('sediment type 1.a' in Vandenberghe (2013)) is a typical component of loess deposits
359 near to or overlying river terraces. Although the NLK section lies on the second terrace of the Kashi
360 River and therefore closer to a potential source of coarser grained material, the fine-sand end
361 member is completely absent. Modal grain sizes in this range (c. 75 um) are common in loess along
362 the Huang Shui and Yellow Rivers in China (Vriend and Prins, 2005;Vandenberghe et al., 2006;Prins
363 et al., 2009), the Danube and Tisza rivers in Serbia (Bokhorst et al., 2011), and the Mississippi valley
364 in the USA (Jacobs et al., 2011). This fraction is generally interpreted to originate from proximal
365 sources, and the grain size of the available source material plays a more important role in
366 determining the grain-size characteristics of this fraction than wind energy (Vandenberghe, 2013).
367 The lack of fine sand at NLK, despite its proximity to the Kashi River, may be attributed to 1) its
368 location in the upper reaches of the river (Fig. 1b), in a region which lacks available ~~stocks-supplies~~
369 of fine sand, 2) the V-shaped nature of the channel which is not conducive to ~~aeolian~~
370 ~~transport~~entrainment of bank deposits, and 3) the relatively high altitude of NLK within the basin
371 which inhibits transport and deposition of coarser sediment grains (Vandenberghe, 2013).

372 The three members (Fig. 3b) identified at NLK correspond to coarse silt (EM1 and EM2) and
373 fine silt (EM3). Each likely represent different kinds of depositional processes which operated
374 throughout the accumulation of the deposit at NLK. Here we focus on the implications of these three

375 end members for understanding past environmental conditions responsible for loess-paleosol
376 sequences formation.

377 EM1 has a modal grain size of 47.5 μm (Fig. 3b), which approximately corresponds to the
378 ‘*subgroup 1.b.1*’ of Vandenberghe (2013). The mode is similar to end members identified in loess
379 from the ~~Chinese Loess Plateau (CLP)~~ and the north-eastern Tibetan Plateau (NE-TP) (EM-2: 44
380 μm) (Vriend et al., 2011). The size of this component is unlikely to be due to longer distance
381 transport. ~~Therefore Rather,~~ it is inferred ~~that EM1 isto~~ derived from shorter distance transport of
382 suspended load (Vriend et al., 2011; Vandenberghe et al., 2006). Coarser particles (~~>20 μm) with~~
383 ~~grain-size >20 μm~~ rarely reach suspension above the near surface level (0 – 200 m above the ground).
384 When entrained by wind, they do not remain in suspension for long enough to travel long distances
385 (Tsoar and Pye, 1987; Pye, 1987). Since the average grain-size of EM1 is 26.74 μm (calculated after
386 Folk and Ward (1957)), we infer that this fraction was transported mainly ~~in-during~~ short-term
387 suspension episodes at lower elevations by surface winds, and deposited short distances downwind
388 of the source. These short-term suspension episodes may correspond to spring-summer dust storms.
389 ~~Our interpretation is supported as demonstrated~~ by present-day dust measurements on the CLP
390 which ~~detected-identify~~ a similar modal grain-size during ~~these-such~~ events (Sun et al 2003).

391 EM2 represents a mode at 33.6 μm (Fig. 3b). It lies towards the finer end of the range of
392 ‘*subgroup 1.b.2*’ (Vandenberghe, 2013). Comparable loess of the same grain size has been identified
393 in loess from the northern Qilian Shan/Hexi Corridor (EM2: 33 μm) ~~in northern China~~, which was
394 also interpreted as depositing from short-term suspension (Nottebaum et al., 2015). Loess of this
395 grain size has been attributed to dust fallout (Pye, 1995; Muhs and Bettis, 2003) and ~~fallout~~ from
396 low-altitude suspension clouds (Sun et al., 2003), as measured from modern depositional events.
397 This fraction requires less wind energy than EM1, is transported further, is more widely distributed,
398 and therefore comprises a higher proportion of the distally ~~deposited-loess~~ populations ~~in-loess~~
399 ~~generally~~ (Vandenberghe, 2013). We propose that EM2 was transported mainly in short-term, near-
400 surface suspension during dust storms, and that wind strength controlled the relative proportions of
401 EM1 and EM2 through time (see the mirror image relationships over millennial scales in Fig. 4).
402 ~~which may implied-This interpretation implies~~ that both EM1 and EM2 have a same origin.

403 The grain-size distribution of EM3 has a modal peak at 18.9 μm (Fig. 3b). This population
404 belongs to ‘*subgroup 1.c.1*’ in Vandenberghe (2013). This population is also widespread in loess
405 from the CLP and ~~NE-TP~~ ~~northeastern Tibetan Plateau~~ (Prins et al., 2007; Prins and Vriend, 2007),
406 ~~and~~ the Danube Basin loess of Europe (Bokhorst et al., 2011; Varga, 2011). ~~It is~~ particularly ~~common~~
407 in loess of interglacial age (Vriend, 2007). There is as yet no consensus ~~as-to~~ ~~regarding~~ the transport
408 processes responsible for this grain size population. On the one hand, researchers have suggested
409 that grains of this size can be lifted by strong vertical air movement and subsequently incorporated
410 into the high-level westerly air streams (Pye, 1995; Pye and Zhou, 1989). This process would link
411 EM3 with long-term suspension transport driven by high-level Westerlies (Prins et al., 2007; Vriend
412 et al., 2011; Nottebaum et al., 2014; Vandenberghe, 2013). Conversely, Zhang et al. (1999) argued
413 that ~~< 20 μm particle fractions~~ ~~EM3~~ derives from “non-dust storm processes” associated with north-
414 westerly surface winds. We argue for the latter on the basis that the EM3 modal grain size from the
415 CLP and ~~northeast Tibetan Plateau~~ ~~NE-TP~~ is coarser (Vriend et al., 2011) than EM3 at NLK in the
416 Ili Valley, which is located further west. If EM3 was transported by high-level westerlies, then one
417 would expect either no significant change (Rea et al., 1985; Rea and Hovan, 1995), or a decrease in
418 grain size from west to east concomitant with wind direction. Furthermore, with mathematical fitting,

419 Sun et al. (2004) related a fine component (2 – 8 μm) to high-altitude westerlies. This fine
420 component is comparable to ‘*subgroup I.c.2*’ of Vandenberghe (2013), which is not consistent with
421 ~~the our~~ modal size of EM3. Observations of modern aeolian processes at the southern margins of
422 the Tarim Basin indicate that fine grain sizes similar to EM3 (8 – 15 μm) are deposited by settling
423 during low velocity wind conditions (Lin et al., 2016). Particle-size distributions of background dust
424 from the northern slopes of the Tianshan Mountains also typically yield a modal peak of
425 approximately 10 μm (Schettler et al., 2014). We therefore infer the EM3 modal peak to derive from
426 low altitude non-dust storm processes.

427 ~~Other possibilities for the deposition of the fine-Fine~~ particles can also be incorporated include
428 ~~the incorporation~~ into silt- or sand-sized aggregates which can be transported by a range of wind
429 velocities, including dust storms (Qiang et al., 2010;Pye, 1995;Derbyshire et al., 1998;Mason et al.,
430 2003). For example, Ujvari et al. (2016) ~~indicated argued~~ that ~~the~~ ~ 1 – 20 μm fractions are affected
431 by aggregation, as shown by comparison between minimally and fully dispersed grain size
432 distributions measurements of loess samples from southern Hungary. Under higher wind velocity
433 conditions, ~~the aggregate model~~ should co-vary with the coarser EM1 particles ~~which were~~
434 transported by surface winds during dust storms. However, since this model is unlikely to hold for
435 EM3 particles (Fig. 4), the aggregate model is ~~not thought unlikely~~ to be responsible for the presence
436 of EM3 grain sizes corresponding to EM3 at NLK.

437 ~~In addition, P~~ost-depositional processes may also influence grain size distribution. In large
438 part this occurs by due to chemical weathering which produces very fine silt and clay minerals (Xiao
439 et al., 1995;Wang et al., 2006;Hao et al., 2008).~~In particular, q~~ Quartz grains are more resistant to
440 ~~weathering-resistant~~ and remain largely unaltered during ~~the~~ post-depositional processes.
441 Consequently, quartz mineral grain size may be used as a more reliable proxy indicator of winter
442 monsoon strength than other components (Sun et al., 2006;Sun et al., 2000b;Xiao et al., 1995).

443 Figure. 6a shows the grain size distribution curves of quartz grains isolated from primary loess
444 (yellow) and paleosol (red) samples. The quartz modal grain size is finer in the paleosol than in the
445 primary loess unit. From this we can deduce that wind strength was weaker during pedogenesis, and
446 stronger during periods of primary loess deposition. The grain size distributions of bulk samples
447 display similar characteristics with those of quartz samples mentioned above (Fig. 6b), ~~whereby~~
448 since soil unit modal peaks (red and orange) are finer than those ~~for in the~~ primary loess (blue and
449 green). Therefore, we argue that wind strength, rather than the post-depositional pedogenesis, has
450 the greatest influence on grain size distribution at NLK, and that EM3 was ~~also~~ not produced by
451 chemical weathering.

452
453 Fig. 6 Comparison of grain size distribution between purified quartz subsamples of paleosol and
454 primary loess (a), and between bulk samples of paleosols and primary loess (b). Comparison of
455 the grain size distribution between EM3 and samples from weak paleosol units (c).

456
457 The relative proportions of the end members down profile can yield ~~further~~ information about
458 temporal variability in wind dynamics. The fairly consistent proportions of EM3 within the loess
459 units indicate it to represent continuous background dust through time (Vandenberghe, 2013).
460 Proportions of EM1 and EM2 decrease noticeably within paleosol units relative to EM3 (Fig. 4).
461 This indicates that variations in proportions of EM3 are mainly driven by variability ~~of in~~ EM1 and
462 EM2 (Vriend et al., 2011), but also that a consistent background sedimentation of EM3 ~~was~~

463 ~~continued dominant~~ during weak pedogenesis (Fig. 6c). This characteristic is comparable with
464 observations from the CLP (Zhang et al., 1999).

465 In addition, small peaks at c. 0.8 μm are also observed in the grain-size distribution curves of
466 all three end members. The generation of ~~these~~ finest grain peaks may be due to post-depositional
467 pedogenesis (Sun, 2006), especially for ~~the~~ particles ~~< with grain size smaller than~~ 2 μm (Bronger
468 and Heinkele, 1990; Sun, 2006). ~~However since the dominant modal peaks are much coarser~~
469 ~~Nevertheless, weaker~~ post-depositional weathering ~~as suggested by MS~~ is unlikely to have had a
470 significant influence on the populations of EM1, EM2 or EM3 ~~at NLK; since the dominant modal~~
471 ~~peaks are much coarser~~. Other potential sources include transportation as aggregates or by the finest
472 grains adhering to coarser particles during transport. Regardless of cause, these particles are unlikely
473 to yield meaningful information about ~~wind regime~~ variability ~~or links to a westerly wind system~~
474 ~~strength climate systems~~ since they do not yield a clear independent end member peak.

475 5.3 Aeolian dust dynamics in eastern Central Asia: links to atmospheric systems

476 Variations in grain size through time at NLK were largely driven by changes in wind strength,
477 without substantial influence of post-depositional pedogenesis. At NLK, grain size ~~is~~ therefore ~~is~~-an
478 indicator ~~for of loess~~ response to ~~the atmospheric climatic~~ systems.

479 The three end members are interpreted to represent different depositional processes which
480 operated throughout the accumulation of the deposit. The finer EM3 is interpreted to represent
481 constant background dust, which continued to accumulate throughout periods of relative stability
482 and pedogenesis. The coarser populations, EM1 and EM2, were transported by low-level winds
483 during major dust storms. EM1 is most likely the most sensitive recorder of wind intensity, since
484 EM2 is less sensitive to wind speeds than EM1 by observation of variations in EM2 proportions
485 throughout LIS1 and LIL2 (Fig. 4).

486
487 Fig. 7 Comparison between EM1 grain size variability ~~with and~~ the timing of glacial advances in
488 the Tien Shan (Koppes et al. 2008; Owen and Dortch, 2014); stable oxygen isotope variations from
489 the Greenland ice cores (Rasmussen et al., 2014); ~~mean grain size (MGS) record of the Jingyuan~~
490 ~~loess section from the CLP (Sun et al., 2010) and; U-ratio (15.6–63.4 $\mu\text{m}/5.61–15.6 \mu\text{m}$) of the SE~~
491 ~~Kazakhstan loess (Machalett et al., 2008), 5-point running average was performed for the intervals~~
492 ~~with higher sedimentary rate on EM1 curve (red line), insolation values at 45°N (Berger and Loutre,~~
493 ~~1991).~~

494
495 From ~~the published~~ OSL data (Song et al., 2015), we used linear regression (Stevens et al.,
496 2016) to construct age–depth relationships over intervals of visually similar sedimentation rate (Fig.
497 S4 and Table S1). ~~Based on the independent chronology sequences, we~~ ~~We~~ ~~assessed~~ the degree of
498 correlation between wind strength variability in the Ili Valley (NLK), as represented by the
499 proportions of EM1, ~~with~~ the stable oxygen isotope record from the Greenland ice cores
500 representing North Atlantic paleoclimate (Rasmussen et al., 2014), ~~the mean grain size (MGS)~~
501 ~~record of the Jingyuan loess section from the CLP (Sun et al., 2010), U-ratio (15.6–63.4 $\mu\text{m}/5.61–$~~
502 ~~15.6 μm) of the Remizovka loess section in SE Kazakhstan (Machalett et al., 2008), and glacial~~
503 ~~advances in the Tien Shan (Owen and Dortch, 2014; Koppes et al., 2008) insolation values at 45°N~~
504 ~~and glacial advances in the Tien Shan~~—(Fig. 7).

505 ~~In Fig. 7,~~ EM1 occurs in ~~larger higher~~ proportions during mid-MIS3, with a higher rate of
506 sedimentary accumulation (Fig. 7). Glaciers ~~in the region~~ expanded during early- and late-MIS3

507 (Owen and Dortch, 2014). ~~The apparent chronological link between increased primary loess~~
508 ~~accumulation and glacial expansion in the region contrasts with trends elsewhere indicating~~
509 ~~increased dust accumulation during dry-windy glacial conditions, and pedogenesis under~~
510 ~~comparatively wetter interglacial conditions. Generally dust is assumed to be generated, and~~
511 ~~deposited, during dry windy glacial conditions, while interglacial conditions were comparatively~~
512 ~~wetter and more conducive to pedogenesis~~ (Stevens et al., 2013; Sun et al., 2010; Ding et al.,
513 2002; Dodonov and Baiguzina, 1995). ~~By contrast, Our observations suggest~~ a seesaw relationship
514 between ~~increased loess accumulation rapid loess deposition~~ and glacial expansion ~~was observed~~
515 during MIS3 ~~from our results~~ (Fig. 7), a model ~~supported that has also been noticed~~ by Youn et al.
516 (2014). ~~The mass accumulation rate (MAR) of loess is good proxy for aridity, while moisture~~
517 ~~Moisture availability appears to be~~ the dominant factor controlling glacier growth in Central Asia,
518 especially for glaciers in the Tian Shan (Zech, 2012; Koppes et al., 2008). We infer, therefore, that
519 moisture had an important impact on accumulation of dust in the study area ~~over during~~ MIS3 in
520 particular.

521 Central Asia is variably influenced by the Asian monsoon from the south (Dettman et al.,
522 2001; Cheng et al., 2012), the mid-latitude westerlies (Vandenberghe et al., 2006), the Siberian high-
523 pressure systems from the northeast (Youn et al., 2014), and the polar front from the north
524 (Machalett et al., 2008). ~~However, by virtue of its geographical position, most of these climate~~
525 ~~influences can be excluded for the Ili Valley since it is sheltered to the northeast, east and south.~~
526 The Asian high mountains largely inhibit the intrusion of Asian (Indian and East Asian) monsoons
527 to the region, ~~since the Ili Valley is sheltered to the northeast, east and south. Studies of the oxygen~~
528 ~~isotopic composition of precipitation in the Tian Shan Mountains region support this geographic~~
529 ~~situation by indicating a stronger connection with westerly circulation than with the Asian summer~~
530 ~~monsoon (Liu et al., 2015; Chen et al., 2016) and the influence of the Siberian High has been shown~~
531 ~~to decrease westward from the CLP.~~

532 Modern satellite data indicates that dust storm development in Ili river valley is closely linked
533 with southward-moving high-latitude air masses (Ye et al., 2003). The large, cold Siberian High
534 pressure system is at the north-northeast of our study area, centring between 40°N and 65°N, 80°E
535 and 120°E (cf. Fig. 3 in Huang et al. (2011)). The Siberian anticyclone dominates winter and spring
536 climate over Eurasia (Sahsamanoglou et al., 1991; Savelieva et al., 2000; Panagiotopoulos et al.,
537 2005; Gong and Ho, 2002; Obrecht et al., 2017). Although the influence of the Siberian High has been
538 shown to decrease westward from the CLP (Vandenberghe et al., 2006), wind strength and frequency
539 over the Aral Sea in western central Asia during the Holocene was nevertheless associated with the
540 intensity of the Siberian High pressure system (Huang et al., 2011; Sorrel et al., 2007). Obrecht et al.
541 (2017) even hypothesized increased influence of the Siberian High during MIS3 over the Lower
542 Danube Basin in SE Europe, although this has yet to be substantiated. Moreover, the Siberian High
543 was considered to be one of the most important influences on dust deposition based on the results
544 of long-term monitoring over Central Asia between 2003 and 2010 (Groll et al., 2013).

545 Increases in modal grain-size from the CLP are also linked to a strengthened East Asian winter
546 monsoon due to intensification of the Siberian High (Ding et al., 1995; Hao et al., 2012). Therefore,
547 the grain-size record from the Chinese loess is a likely indicator of Siberian High intensity. We use
548 the Jingyuan loess section as a point of comparison in our study, because it is a high resolution
549 record located in the northwestern CLP, with high sedimentation rate, and thus the likelihood of

550 preservation of millennial-scale oscillations. We compared secular trends between the EM1
551 proportions and MGS data from Jingyuan over the last glacial period (Sun et al., 2010). Similarities
552 can be observed (Fig. 7); coarser grain sizes and higher sedimentation rates are observed during
553 mid-MIS3 (Sun et al., 2010), with the opposite occurring in early- and late-MIS3. This supports a
554 common Eurasian atmospheric forcing pattern - the Siberian High - driving the climate evolution of
555 the Ili Basin and CLP during that time period.

556 By comparison, the Last Glacial Maximum (LGM) witnesses significantly different trends,
557 despite increased sedimentation rates (Sun et al., 2010) (Fig. 7). EM1 proportions decrease
558 particularly during the early-LGM. We attribute this to a reduction in sediment supply, possibly
559 linked to permafrost development in the Ili Basin and Kazakhstan steppe (Fig. 1) (Zhao et al.,
560 2014; Vandenberghe et al., 2014). Reduced sediment supply therefore limits the degree to which
561 grain-size characteristics can reliably indicate wind strength during the LGM.

562 Machalett et al. (2008), presenting data from the Remizovka site in the more open western Ili
563 Basin, argued that the Arctic polar front, expanding southward in winter and retracting northward
564 in summer, most likely increased the frequency and strength of cyclonic storms due to higher
565 temperature and humidity gradients created between colder polar air and warmer tropical air
566 (Harman, 1991). They hypothesized that this climate system was the predominant influence on dust
567 transport and loess accumulation during cold phases along the Kyrgyz (southern) Tian Shan
568 piedmont. While this may have been the case at Remizovka, it is unlikely to have affected NLK in
569 the eastern Ili Basin, however, since the eastern basin is much more sheltered due to the position of
570 the mountain ranges (Fig. 1a).

571 To assess spatial variability in climatic influence across the Ili Basin, we compare EM1 curve
572 with U-ratio (15.6–63.4 μm /5.61–15.6 μm) of the polar-front-influenced Remizovka loess. We
573 observe minimal similarities in the curves. These disparities suggest that two different atmospheric
574 forcing patterns controlled loess accumulation from one end of the Ili Basin to the other. The
575 differences appear to be particularly clear over MIS3, respectively (Fig. 7), although problems with
576 chronological integrity at the Remizovka site need to be resolved (Fitzsimmons et al., 2016) before
577 we can argue this with confidence. In addition, U-ratios decrease during the LGM (Fig. 7),
578 supporting our hypothesis that the development of permafrost limits the availability of source
579 sediments for loess in this region.

580 We argue that the Siberian high-pressure system exerts a significant influence on wind
581 dynamics and loess deposition in the eastern Ili Basin. It is evident that the strongest winds at NLK
582 site mainly blow from the west (Table S2), although northerly high-latitude air masses with potential
583 for short-term dust transport can enter the Ili Basin by deflection around the northern Tian Shan (Fig.
584 S5).

585 Enhanced evaporation, coupled with strengthened westerly winds, would bring more humid
586 and warmer conditions to ACA during the Holocene (Zhang et al., 2016). Karger et al. (2016)
587 reconstructed the dynamics of the westerlies in the Ili Basin, proposing a rain belt which seasonally
588 migrates towards the south and north in autumn and summer, respectively. A strengthened Siberian
589 High would push the mid-latitude Westerlies pathways further to the south, resulting in comparably
590 drier conditions in northeastern Central Asia (e.g. Tian Shan) but wetter conditions in southwestern
591 Central Asia (Pamir) (Lei et al., 2014; Wolff et al., 2017). The intensity and geographical position of
592 the Siberian High would most likely impact precipitation and atmospheric circulation patterns
593 (meridional or zonal) in the mid-latitudes Central Asian (Panagiotopoulos et al., 2005). It is

594 therefore most likely that, the mid-latitude Westerlies controlled broad-scale patterns of moisture
595 variation across ACA broadly (Huang et al., 2015; Li et al., 2011; Cai et al., 2017), whereas the
596 eastern Ili Basin experienced the combined influence of the Siberian High and the mid-latitude
597 Westerlies system.

598 Modern satellite data indicates that dust storm development in Ili river valley is closely linked
599 with southward-moving high-latitude air masses. — provided a detailed picture of the westerlies for
600 the Ili Basin, in which a rain belt gradually migrated towards the south and north in autumn and
601 summer, respectively. According to this scenario, enhanced evaporation coupled with strengthened
602 westerly winds would bring more humid and warm air masses to Arid Central Asia (ACA) during
603 the Holocene. Therefore, based on our grain size observations, we argue that the Arctic polar front,
604 intruding southward in the winter and retracting northward in summer, most likely increased the
605 frequency and strength of cyclonic storms, leading to dust transport and the accumulation of loess
606 deposits during cold phases when it predominated in the Ili Basin and along the Kyrgyz Tian Shan
607 piedmont. While the mid-latitude westerlies increasingly influenced the climate in this region as the
608 climate became warmer when the polar front shifted northward, and controlled the patterns of
609 moisture variations.

610 Comparison of EM1 proportions with variability in June insolation at 45°N shows a distinct
611 correlative relationship on the orbital timescale (Fig. 7), which indicates local insolation-based
612 control on wind dynamics. When the insolation values increases, the rising of temperature, as a
613 result, enhances the frequency or strength of cyclonic storms, resulting in higher sedimentary rates
614 or higher coarse-grain proportions (Fig. 7). However, EM1 proportions exhibit more substantial
615 fluctuations than may be attributed to insolation values during the mid- and late MIS3. We ascribe
616 that to the humidity variations in the study area. In the early-MIS 3, increased moistures due to
617 migration of westerlies towards the north were conducive to vegetation growth in source areas,
618 which reduced sediment entrainment and resulted in less contribution of coarse grains to loess site,
619 though glacial grinding of rocks in the high mountains could produce amount of fine-grained
620 materials. Whereas arid environment in the mid-MIS 3, observed by a lack of glacial advance in
621 Tian Shan (Fig. 7) and also reflected by the increased MAR (Fig. 7), likely made these sediments
622 with coarser grain size produced in the early-MIS 3 available as the source materials for NLK loess,
623 as the case in the north-eastern Tibetan Plateau.

624 Over millennial scales, our grain size proxy data do not correlate strongly with abrupt events,
625 such as H1, H2, H3 and H5, identified from the North Atlantic records (Fig. 7). Some of the peaks
626 in EM1 curve correspond to valleys in GISP $\delta^{18}\text{O}$ curve (black arrows in Fig. 7), yet many do not.

627 Grain size studies of the Darai Kalon loess section in Tajikistan, 1200 km to the southwest of
628 NLK, inferred a strong influence from the westerlies resulting in transport of the North Atlantic
629 signal to the East Asia. Darai Kalon is, however, located in a region where the mid-latitude
630 westerlies clearly have a much stronger influence. Our results from the Ili Basin contradict those of,
631 which suggest that the mid-latitude westerlies probably did not predominate north of the Kyrgyz
632 Tian Shan. In this case, the high mountains in Central Asia most likely obstructed the migration of
633 the Asiatic polar front further south towards Tajikistan where those data were derived, thereby
634 resulting in a stronger westerlies signal at Darai Kalon than at NLK.

635 Our results also contradict those of, who proposed that millennial-scale North Atlantic climate
636 signals might have been transmitted to the Siberian High via the Barents and Kara Sea ice sheets,
637 and then propagated eastwards to the Chinese Loess Plateau via the winter monsoon system. In our

638 ease, the influence from northern climate subsystems such as the Siberian High or polar front appear
639 ~~not to have transmitted millennial scale North Atlantic climatic events, maybe supporting the~~
640 ~~significance of the westerlies in transmitting North Atlantic climate signals to East Asia.~~

641 Comparison of EM1 proportions with variability in GISP $\delta^{18}\text{O}$ suggests that our grain-size
642 proxy data may correlate with abrupt events, such as North Atlantic Heinrich events H1 to H6 (Fig.
643 7), ~~although this correlation cannot yet be better constrained due to limitations in the chronological~~
644 ~~dataset. Some of the peaks in EM1 curve correspond to troughs in GISP $\delta^{18}\text{O}$ curve (black arrows~~
645 ~~in Fig. 7) outside Heinrich events, yet many do not (pink dashed lines in Fig. 7). Potential causes of~~
646 ~~this discrepancy may lie in variability in local source availability and wind dynamics at certain~~
647 ~~points in time.~~

648 Comparisons between the eastern Ili Basin and Chinese Loess Plateau loess further elucidates
649 complexity in the climatic signal preserved in the ACA. The NLK EM1 proportions in the Ili Basin
650 yield lower variability than the Jingyuan MGS on the CLP, particularly during H2 and H5 (Fig. 7).
651 We attribute these differences to local source sediment availability at NLK. EM1 supply to NLK
652 was reduced during H2 due to the development of permafrost, and during H5 due to increased
653 vegetation cover associated with more humid conditions inhibiting coarse-grain entrainment (Fig.
654 7). By contrast, the relatively more arid mid-MIS 3, indicated by glacial retreat in the Tian Shan,
655 may have decreased vegetation cover and increased entrainment potential and transport to NLK (Fig.
656 7); these conditions and this trend was also observed in the NE-TP (Vriend et al., 2011). The
657 differences may be because the loess records in our study area represent a response not only to
658 hemispheric climate systems, but also to local influences such as local atmospheric circulation and
659 topography. Since the sedimentary response to changing climate conditions in more arid Central
660 Asia is different to that of the more temperate European loess (Rousseau et al., 2007), we must be
661 careful about investigating the mechanisms of aeolian dynamics and loess accumulation in our
662 paleoclimatic interpretations of ACA loess archives.

663 Many studies have speculate that millennial-scale oscillations represent a teleconnection
664 between the North Atlantic and East Asia (e.g. Porter and An, 1995; Yang and Ding, 2014), although
665 the dynamics involved are poorly understood. Porter and An (1995) and Sun et al. (2012) suggested,
666 based on CLP loess physical characteristics, that a strong influence from the westerlies resulted in
667 transport of the North Atlantic signal to East Asia. Conversely, Yang and Ding (2014) proposed that
668 millennial-scale North Atlantic climate signals might have been transmitted to the Siberian High via
669 the Barents and Kara Sea ice sheets, and were propagated eastwards to the CLP via the winter
670 monsoon system. In the western CLP (Chen et al., 1997a), for example, evidence of millennial-scale
671 (likely Heinrich) events are preserved within the loess stratigraphy during phases of strong winter
672 monsoon in China; however, not all of the strong winter monsoon events in China correlate with
673 Heinrich events in the North Atlantic, so challenging the Yang and Ding (2014) hypothesis.

674 Stronger datasets from Central Asia may provide the missing link for understanding climate
675 teleconnections between the two extreme ends of the Eurasian continent. In doing so, however, the
676 scale of the “Central Asian” region must be taken into account. At Darai Kalon in Tajikistan, 1200
677 km southwest of NLK, the mid-latitude westerlies clearly have a strong influence on dust transport
678 and loess accumulation; Atlantic signals are clearly identified in grain size variations, especially
679 during full glacial phases (Vandenberghe et al., 2006). Since the CLP lies at a similar latitude to
680 Darai Kalon, mid-latitude Westerlies have the potential to transport North Atlantic climate signals
681 to East Asia. By contrast, since NLK is located substantially further north than Darai Kalon and the

带格式的: 缩进: 首行缩进: 0 字符

682 CLP, the Siberian High exerts a greater influence on wind dynamics and therefore loess deposits. A
683 strengthened Siberian High would effect a southward shift of the mid-latitude Westerlies pathways;
684 under such conditions, NLK would be less strongly influenced by the mid-latitude westerlies. This
685 argument is further supposed by the lack of correlation between NLK EM1 proportions and GISP
686 $\delta^{18}\text{O}$ values during relatively mild interstadial periods (Dansgaard-Oeschger cycles) when the mid-
687 latitude westerlies shift northwards (Fig. 7). Therefore, NLK provides a strategic location for
688 investigating the potential role of the Siberian High in transmitting North Atlantic climate signals
689 to East Asia. The preservation of North Atlantic several millennial-scale Heinrich events at NLK
690 supports the argument for the influence of the Siberian High as argued by Yang and Ding (2014).

691 **Conclusion**

692 ~~In this study, Our data from NLK in the eastern Ili Basin provides a paleoenvironmental record~~
693 ~~over the last c. 70 ky for the last glacial from the Nilka (NLK) loess section in Ili Basin was provided.~~
694 The magnetic properties of the loess do not correlate with ~~indicate that no strong~~ pedogenesis
695 ~~occurred in this section; rather, even in the paleosol units. Variations in magnetic susceptibility (MS)~~
696 ~~value closely correlate with the proportions of sand fraction, and, wind strength is mainly~~
697 responsible for ~~those~~ variations in physical characteristics ~~since over~~ the last glacial period.

698 ~~With the unmixing of grain size distributions, t~~Three grain-size end members were
699 distinguished/identified at NLK: EM1 (mode size at 47.5 μm), EM2 (33.6 μm) and EM3 (18.9 μm).
700 They are indicative of different kinds of depositional processes which operated throughout the
701 accumulation of the loess ~~deposit at NLK section~~. EM1 and EM2 represented ~~the~~ grain-size fractions
702 transported from proximal sources in short-term, near-surface suspension during dust outbreaks.
703 ~~They, and~~ may have the same origin. While wind strength ~~their~~ controls relative proportions, EM1
704 is ~~most likely~~ the most sensitive recorder of wind strength. EM3 represents continuous background
705 dust under ~~the non-~~dust storm processes.

706 The Siberian High-pressure system predominates in the eastern Ili Basin during cold phases,
707 which leads to dust transport and increased loess accumulation at NLK. Many rapid cooling events,
708 including 6 Heinrich events, were imprinted in the NLK loess. Our grain-size data support the
709 argument that the Siberian High plays a significant role in transporting North Atlantic climatic
710 signals to East Asia via ice sheets in the high northern latitudes.

711 ~~The Arctic polar front predominates in the Ili Basin and the Kyrgyz-Tian Shan piedmont during~~
712 ~~cold phases, which leads to the dust transport and increased accumulation of loess deposits, while~~
713 ~~the shift of mid-latitude westerlies towards the south and north controlled the patterns of~~
714 ~~precipitation/moisture variations in this region. On the orbital scale, the local insolation-based~~
715 ~~control has an important impact on wind dynamics directly related to accumulation of loess, and~~
716 ~~moisture can may also influence grain size of loess in the study area over MIS3 in particular.~~
717 ~~Although, the polar front dominated wind dynamics for loess deposition in the Ili Basin and the~~
718 ~~Kyrgyz-Tian Shan, the Central Asian high mountains obstructed its migration further south. Our~~
719 ~~results may also support the significance of the mid-latitude westerlies in transmitting North Atlantic~~
720 ~~climate signals to East Asia.~~

721 **Acknowledgements**

722 The project is supported by the National Basic Research Program of China (Nos:
723 2016YFA0601902, 2013CB955904), Natural Science Foundation of China (Nos: 41572162,
724 41290253), and International ~~partnership~~ Partnership Program of Chinese Academy of Science [No:
725 132B61KYS20160002]. The authors thank Yun Li and Junchao Dong from Institute of Earth

726 Environment, Chinese Academy of Sciences, for their assistances in sampling and experiment, and
727 Jia Li from Xiamen University for her assistance in mathematical treatment.

728 References

- 729 Antoine, P., Rousseau, D.-D., Moine, O., Kunesch, S., Hatté, C., Lang, A., Tissoux, H., and Zöller,
730 L.: Rapid and cyclic aeolian deposition during the Last Glacial in European loess: a high-resolution
731 record from Nussloch, Germany, *Quaternary Sci Rev*, 28, 2955-2973, 2009.
- 732 Beget, J. E., and Hawkins, D. B.: Influence of Orbital Parameters on Pleistocene Loess Deposition
733 in Central Alaska, *Nature*, 337, 151-153, DOI 10.1038/337151a0, 1989.
- 734 Bokhorst, M. P., Vandenberghe, J., Sumegi, P., Lanczont, M., Gerasimenko, N. P., Matviishina, Z.
735 N., Markovic, S. B., and Frechen, M.: Atmospheric circulation patterns in central and eastern
736 Europe during the Weichselian Pleniglacial inferred from loess grain-size records, *Quatern Int*, 234,
737 62-74, 10.1016/j.quaint2010.07.018, 2011.
- 738 Bond, G., Heinrich, H., Broecker, W., Labeyrie, L., Mcmanus, J., Andrews, J., Huon, S., Jantschik,
739 R., Clasen, S., Simet, C., Tedesco, K., Klas, M., Bonani, G., and Ivy, S.: Evidence for massive
740 discharges of icebergs into the North Atlantic Ocean during the last glacial period, *Nature*, 360,
741 245–249, 1992.
- 742 Bronger, A., and Heinkele, T.: Mineralogical and clay mineralogical aspects of loess research,
743 *Quatern Int*, 7, 37-51, 1990.
- 744 Buggle, B., Hambach, U., Glaser, B., Gerasimenko, N., Markovic, S., Glaser, I., and Zöller, L.:
745 Stratigraphy, and spatial and temporal paleoclimatic trends in Southeastern/Eastern European loess-
746 paleosol sequences, *Quatern Int*, 196, 86–106, 2009.
- 747 Buggle, B., Hambach, U., Muller, K., Zoller, L., Markovic, S. B., and Glaser, B.: Iron mineralogical
748 proxies and Quaternary climate change in SE-European loess-paleosol sequences, *Catena*, 117, 4-
749 22, 10.1016/j.catena.2013.06.012, 2014.
- 750 Cai, Y. J., Chiang, J. C. H., Breitenbach, S. F. M., Tan, L. C., Cheng, H., Edwards, R. L., and An, Z.
751 S.: Holocene moisture changes in western China, Central Asia, inferred from stalagmites,
752 *Quaternary Sci Rev*, 158, 15-28, 2017.
- 753 Chen, F., Bloemendal, J., Wang, J., Li, J., and Oldfield, F.: High-resolution multi-proxy climate
754 records from Chinese loess: evidence for rapid climatic changes over the last 75 kyr,
755 *Palaeogeography, Palaeoclimatology, Palaeoecology*, 130, 323-335, 1997a.
- 756 Chen, F. H., Bloemendal, J., Wang, J. M., Li, J. J., and Oldfield, F.: High-resolution multi-proxy
757 climate records from Chinese loess, evidence for rapid climatic changes over the last 75 kyr,
758 *Palaeogeogr Palaeoclimatol*, 130, 323-335, 1997b.
- 759 Chen, F. H., Jia, J., Chen, J. H., Li, G. Q., Zhang, X. J., Xie, H. C., Xia, D. S., Huang, W., and An,
760 C. B.: A persistent Holocene wetting trend in arid central Asia, with wettest conditions in the late
761 Holocene, revealed by multi-proxy analyses of loess-paleosol sequences in Xinjiang, China,
762 *Quaternary Sci Rev*, 146, 134-146, 2016.
- 763 Cheng, H., Zhang, P. Z., Spotl, C., Edwards, R. L., Cai, Y. J., Zhang, D. Z., Sang, W. C., Tan, M.,
764 and An, Z. S.: The climatic cyclicity in semiarid-arid central Asia over the past 500,000 years,
765 *Geophys Res Lett*, 39, Artn L01705
766 10.1029/2011gl050202, 2012.
- 767 Dansgaard, W., Johnsen, S. J., Clausen, H. B., Hvidberg, C. S., and Steffensen, J. P.: Evidence for
768 general instability of past climate from a 250-kyr ice-core record, *Nature*, 364, 218– 220, 1993.
- 769 Derbyshire, E., Meng, X. M., and Kemp, R. A.: Provenance, transport and characteristics of modern

域代码已更改

带格式的: 字体: (默认) Times New Roman, 五号

770 aeolian dust in western Gansu Province, China, and interpretation of the Quaternary loess record,
771 *Journal of Arid Environments*, 39, 497-516, DOI 10.1006/jare.1997.0369, 1998.

772 Dettman, D. L., Kohn, M. J., Quade, J., Ryerson, F. J., Ojha, T. P., and Hamidullah, S.: Seasonal
773 stable isotope evidence for a strong Asian monsoon throughout the past 10.7 m.y., *Geology*, 29, 31-
774 34, Doi 10.1130/0091-7613(2001)029<0031:Ssiefa>2.0.Co;2, 2001.

775 Ding, Z., Liu, T., Rutter, N. W., Yu, Z., Guo, Z., and Zhu, R.: Ice-volume forcing of East Asian
776 winter monsoon variations in the past 800,000 years, *Quaternary Res*, 44, 149-159, 1995.

777 Ding, Z. L., Sun, J. M., Rutter, N. W., Rokosh, D., and Liu, T. S.: Changes in sand content of loess
778 deposits along a north-south transect of the Chinese Loess Plateau and the implications for desert
779 variations, *Quaternary Research*, 52, 56-62, DOI 10.1006/qres.1999.2045, 1999.

780 Ding, Z. L., Ranov, V., Yang, S. L., Finaev, A., Han, J. M., and Wang, G. A.: The loess record in
781 southern Tajikistan and correlation with Chinese loess, *Earth Planet Sc Lett*, 200, 387-400, doi: DOI:
782 10.1016/S0012-821X(02)00637-4, 2002.

783 Ding, Z. L., Derbyshire, E., Yang, S. L., Sun, J. M., and Liu, T. S.: Stepwise expansion of desert
784 environment across northern China in the past 3.5 Ma and implications for monsoon evolution,
785 *Earth Planet Sc Lett*, 237, 45-55, 10.1016/j.epsl.2005.06.036, 2005.

786 DiPietro, L. M., Driese, S. G., Nelson, T. W., and Harvill, J. L.: Variations in late Quaternary wind
787 intensity from grain-size partitioning of loess deposits in the Nenana River Valley, Alaska,
788 *Quaternary Research*, 87, 258-274, 2017.

789 Dodonov, A. E., and Baiguzina, L. L.: Loess stratigraphy of Central Asia: Palaeoclimatic and
790 palaeoenvironmental aspects, *Quaternary Sci Rev*, 14, 707-720, [http://dx.doi.org/10.1016/0277-
791 3791\(95\)00054-2](http://dx.doi.org/10.1016/0277-3791(95)00054-2), 1995.

792 Dodonov, A. E., Sadchikova, T. A., Sedov, S. N., Simakova, A. N., and Zhou, L. P.:
793 Multidisciplinary approach for paleoenvironmental reconstruction in loess-paleosol studies of the
794 Darai Kalon section, Southern Tajikistan, *Quatern Int*, 152, 48-58, 10.1016/j.quaint.2005.12.001,
795 2006.

796 Feng, Z. D., Ran, M., Yang, Q. L., Zhai, X. W., Wang, W., Zhang, X. S., and Huang, C. Q.:
797 Stratigraphies and chronologies of late Quaternary loess-paleosol sequences in the core area of the
798 central Asian arid zone, *Quatern Int*, 240, 156-166, doi: 10.1016/j.quaint.2010.10.019, 2011.

799 Fitzsimmons, K. E., Sprafke, T., Zielhofer, C., Günter, C., Deom, J. M., Sala, R., and Iovita, R.:
800 Loess accumulation in the Tian Shan piedmont: Implications for palaeoenvironmental change in
801 arid Central Asia, *Quatern Int*, <http://dx.doi.org/10.1016/j.quaint.2016.1007.1041>, 2016.

802 Folk, R. L., and Ward, W. C.: Brazos River bar: a study in the significance of grain size parameters,
803 *Journal of Sedimentary Research*, 27, 3-26, 1957.

804 Gong, D. Y., and Ho, C. H.: The Siberian High and climate change over middle to high latitude Asia,
805 *Theor Appl Climatol*, 72, 1-9, 2002.

806 Grimley, D. A., and Arruda, N. K.: Observations of magnetite dissolution in poorly drained soils,
807 *Soil Sci*, 172, 968-982, 10.1097/ss.0b013e3181586b77, 2007.

808 Groll, M., Opp, C., and Aslanov, I.: Spatial and temporal distribution of the dust deposition in
809 Central Asia - results from a long term monitoring program, *Aeolian Res*, 9, 49-62, 2013.

810 Hao, Q., Wang, L., Oldfield, F., Peng, S., Qin, L., Song, Y., Xu, B., Qiao, Y., Bloemendal, J., and
811 Guo, Z.: Delayed build-up of Arctic ice sheets during 400,000-year minima in insolation variability,
812 *Nature*, 490, 393-396, 2012.

813 Hao, Q. Z., Oldfield, F., Bloemendal, J., and Guo, Z. T.: Particle size separation and evidence for

814 pedogenesis in samples from the Chinese Loess Plateau spanning the past 22 m.y., *Geology*, 36,
815 727-730, 2008.

816 Harman, J. R.: *Synoptic Climatology of the Westerlies: Process and Patterns*, Association of
817 American Geographers, Washington, DC, 1991.

818 Heller, F., and Liu, T. S.: Magnetism of Chinese Loess Deposits, *Geophys J Roy Astr S*, 77, 125-&,
819 DOI 10.1111/j.1365-246X.1984.tb01928.x, 1984.

820 Heller, F., Shen, C. D., Beer, J., Liu, X. M., Liu, T. S., Bronger, A., Suter, M., and Bonani, G.:
821 Quantitative Estimates of Pedogenic Ferromagnetic Mineral Formation in Chinese Loess and
822 Paleoclimatic Implications, *Earth Planet Sc Lett*, 114, 385-390, Doi 10.1016/0012-821x(93)90038-
823 B, 1993.

824 Heller, F., and Evans, M. E.: Loess magnetism, *Reviews of Geophysics*, 33, 211-240, 1995.

825 Huang, W., Chen, J. H., Zhang, X. J., Feng, S., and Chen, F. H.: Definition of the core zone of the
826 "westerlies-dominated climatic regime", and its controlling factors during the instrumental period,
827 *Science China-Earth Sciences*, 58, 676-684, 10.1007/s11430-015-5057-y, 2015.

828 Huang, X. T., Oberhansli, H., von Suchodoletz, H., and Sorrel, P.: Dust deposition in the Aral Sea:
829 implications for changes in atmospheric circulation in central Asia during the past 2000 years,
830 *Quaternary Sci Rev*, 30, 3661-3674, 2011.

831 Jacobs, P. M., Mason, J. A., and Hanson, P. R.: Mississippi Valley regional source of loess on the
832 southern Green Bay Lobe land surface, Wisconsin, *Quaternary Research*, 75, 574-583,
833 10.1016/j.yqres.2011.02.003, 2011.

834 Jia, J., Xia, D. S., Wei, H. T., Wang, B., and Liu, X. B.: A magnetic investigation of a loess/paleosol
835 sequences record in Ili area, *Front Earth Sci-Prc*, 4, 259-268, 10.1007/s11707-010-0115-4, 2010.

836 Jia, J., Xia, D. S., Wang, B., Wei, H. T., and Liu, X. B.: Magnetic investigation of Late Quaternary
837 loess deposition, Ili area, China, *Quatern Int*, 250, 84-92, 10.1016/j.quaint.2011.06.018, 2012.

838 Karger, D. N., Conrad, O., Böhrer, J., Kawohl, T., Kreft, H., Soria-Auza, R. W., Zimmermann, N.,
839 Linder, H. P., and Kessler, M.: Climatologies at high resolution for the Earth land surface areas,
840 arXiv:1607.00217, 2016.

841 Konert, M., and Vandenberghe, J.: Comparison of laser grain size analysis with pipette and sieve
842 analysis: A solution for the underestimation of the clay fraction, *Sedimentology*, 44, 523-535, DOI
843 10.1046/j.1365-3091.1997.d01-38.x, 1997.

844 Koppes, M., Gillespie, A. R., Burke, R. M., Thompson, S. C., and Stone, J.: Late Quaternary
845 glaciation in the Kyrgyz Tien Shan, *Quaternary Sci Rev*, 27, 846-866,
846 10.1016/j.quascirev.2008.01.009, 2008.

847 Lei, Y. B., Tian, L. D., Bird, B. W., Hou, J. Z., Ding, L., Oimahmadov, I., and Gadoev, M.: A 2540-
848 year record of moisture variations derived from lacustrine sediment (Sasikul Lake) on the Pamir
849 Plateau, *Holocene*, 24, 761-770, 2014.

850 Li, G. Q., Rao, Z. G., Duan, Y. W., Xia, D. S., Wang, L. B., Madsen, D. B., Jia, J., Wei, H. T., Qiang,
851 M. R., Chen, J. H., and Chen, F. H.: Paleoenvironmental changes recorded in a luminescence dated
852 loess/paleosol sequence from the Tianshan Mountains, arid central Asia, since the Penultimate
853 Glaciation, *Earth Planet Sc Lett*, 448, 1-12, 10.1016/j.epsl.2016.05.008, 2016a.

854 Li, J.: *Climate in Xinjiang*, in: China Meteorological Press, Beijing, 1-205 (in Chinese), 1991.

855 Li, X., Zhao, K., Dodson, J., and Zhou, X.: Moisture dynamics in central Asia for the last 15 kyr:
856 new evidence from Yili Valley, Xinjiang, NW China, *Quaternary Sci Rev*, 30, 3457-3466, 2011.

857 Li, Y., Song, Y., Lai, Z., Han, L., and An, Z.: Rapid and cyclic dust accumulation during MIS 2 in

858 Central Asia inferred from loess OSL dating and grain-size analysis, *Scientific Reports*, 6, DOI:
859 10.1038/srep32365, 2016b.

860 Li, Y., Song, Y. G., Chen, X. L., Li, J. C., Mamadjanov, Y., and Aminov, J.: Geochemical
861 composition of Tajikistan loess and its provenance implications, *Palaeogeogr Palaeocl*, 446, 186-
862 194, 10.1016/j.palaeo.2016.01.025, 2016c.

863 Lin, Y. C., Mu, G. J., Xu, L. S., and Zhao, X.: The origin of bimodal grain-size distribution for
864 aeolian deposits, *Aeolian Research*, 20, 80-88, 10.1016/j.aeolia.2015.12.001, 2016.

865 Liu, Q. S., Deng, C. L., Torrent, J., and Zhu, R. X.: Review of recent developments in mineral
866 magnetism of the Chinese loess, *Quaternary Sci Rev*, 26, 368-385, 10.1016/j.quascirev.2006.08.004,
867 2007.

868 Liu, Q. S., Roberts, A. P., Larrasoana, J. C., Banerjee, S. K., Guyodo, Y., Tauxe, L., and Oldfield,
869 F.: *Environmental Magnetism: Principles and Applications*, *Reviews of Geophysics*, 50, Artn
870 Rg4002
871 10.1029/2012rg000393, 2012.

872 Liu, T.: *Loess and the Environment* (In Chinese), China Ocean Press, Beijing, 251 pp., 1985a.

873 Liu, T. S.: *Loess and the environment*, Ocean Press, Beijing, 1985b.

874 Liu, X., Liu, Z., Lü, B., Marković, S., Chen, J., Guo, H., Ma, M., Zhao, G., and Feng, H.: The
875 magnetic properties of Serbian loess and its environmental significance, *Chinese Science Bulletin*,
876 1-11, 2013.

877 Liu, X. K., Rao, Z. G., Zhang, X. J., Huang, W., Chen, J. H., and Chen, F. H.: Variations in the
878 oxygen isotopic composition of precipitation in the Tianshan Mountains region and their
879 significance for the Westerly circulation, *J Geogr Sci*, 25, 801-816, 2015.

880 Liu, X. M., Shaw, J., Liu, T. S., Heller, F., and Yuan, B. Y.: Magnetic Mineralogy of Chinese Loess
881 and Its Significance, *Geophys J Int*, 108, 301-308, DOI 10.1111/j.1365-246X.1992.tb00859.x, 1992.

882 Liu, X. M., Rolph, T., Bloemendal, J., Shaw, J., and Liu, T. S.: Remanence characteristics of
883 different magnetic grain size categories at Xifeng, central Chinese Loess Plateau, *Quaternary
884 Research*, 42, 162-165, 1994.

885 Liu, X. M., Hesse, P., Rolph, T., and Begét, J. E.: Properties of magnetic mineralogy of Alaskan
886 loess: evidence for pedogenesis, *Quatern Int*, 62, 93-102, 1999.

887 Lu, H. Y., and An, Z. S.: Pretreatment methods in loess-palaeosol granulometry, *Chinese Science
888 Bulletin*, 42, 237-240, 1997.

889 Lu, H. Y., and An, Z. S.: Paleoclimatic significance of grain size of loess-palaeosol deposit in
890 Chinese Loess Plateau, *Sci China Ser D*, 41, 626-631, Doi 10.1007/Bf02878745, 1998.

891 Machalet, B., Frechen, M., Hambach, U., Oches, E. A., Zoller, L., and Markovic, S. B.: The loess
892 sequence from Remisowka (northern boundary of the Tien Shan Mountains, Kazakhstan) - Part I:
893 Luminescence dating, *Quatern Int*, 152, 192-201, 10.1016/j.quaint.2005.12.014, 2006.

894 Machalet, B., Oches, E. A., Frechen, M., Zoller, L., Hambach, U., Mavlyanova, N. G., Markovic,
895 S. B., and Endlicher, W.: Aeolian dust dynamics in central Asia during the Pleistocene: Driven by
896 the long-term migration, seasonality, and permanency of the Asiatic polar front, *Geochem Geophys
897 Geosy*, 9, Artn Q08q09
898 10.1029/2007gc001938, 2008.

899 Maher, B., and Thompson, R.: Paleoclimatic significance of the mineral magnetic record of the
900 Chinese loess and paleosols, *Quaternary Research*, 37, 155-170, 1992.

901 Maher, B. A., and Taylor, R. M.: Formation of Ultrafine-Grained Magnetite in Soils, *Nature*, 336,

902 368-370, DOI 10.1038/336368a0, 1988.

903 Maher, B. A., and Thompson, R.: Paleorainfall reconstructions from pedogenic magnetic
904 susceptibility variations in the Chinese loess and paleosols, *Quaternary Research*, 44, 383-391, DOI
905 10.1006/qres.1995.1083, 1995.

906 Maher, B. A.: Magnetic properties of modern soils and Quaternary loessic paleosols: paleoclimatic
907 implications, *Palaeogeogr Palaeocl*, 137, 25-54, Doi 10.1016/S0031-0182(97)00103-X, 1998.

908 Maher, B. A.: Palaeoclimatic records of the loess/palaeosol sequences of the Chinese
909 Loess Plateau, *Quaternary Sci Rev*, 154, 23-84, 2016.

910 Mason, J. A., Jacobs, P. M., Greene, R. S. B., and Nettleton, W. D.: Sedimentary aggregates in the
911 Peoria Loess of Nebraska, USA, *Catena*, 53, 377-397, 10.1016/S0341-8162(03)00073-0, 2003.

912 Muhs, D. R., and Bettis, E. A.: Quaternary loess-paleosol sequences as examples of climate-driven
913 sedimentary extremes, *Special Papers-Geological Society of America*, 53-74, 2003.

914 Muhs, D. R.: The geologic records of dust in the Quaternary, *Aeolian Research*, 9, 3-48, 2013.

915 Nawrocki, J., Wojcik, A., and Bogucki, A.: The magnetic susceptibility record in the Polish and
916 western Ukrainian loess-palaeosol sequences conditioned by palaeoclimate, *Boreas*, 25, 161-169,
917 1996.

918 Nottebaum, V., Lehmkuhl, F., Stauch, G., Hartmann, K., Wunnemann, B., Schimpf, S., and Lu, H.
919 Y.: Regional grain size variations in aeolian sediments along the transition between Tibetan
920 highlands and north-western Chinese deserts - the influence of geomorphological settings on aeolian
921 transport pathways, *Earth Surf Proc Land*, 39, 1960-1978, 10.1002/esp.3590, 2014.

922 Nottebaum, V., Stauch, G., Hartmann, K., Zhang, J. R., and Lehmkuhl, F.: Unmixed loess grain size
923 populations along the northern Qilian Shan (China): Relationships between geomorphologic,
924 sedimentologic and climatic controls, *Quatern Int*, 372, 151-166, 10.1016/j.quaint.2014.12.071,
925 2015.

926 Obreht, I., Zeeden, C., Schulte, P., Hambach, U., Eckmeier, E., Timar-Gabor, A., and Lehmkuhl, F.:
927 Aeolian dynamics at the Orlovat loess-paleosol sequence, northern Serbia, based on detailed textural
928 and geochemical evidence, *Aeolian Research*, 18, 69-81, 2015.

929 Obreht, I., Hambach, U., Veres, D., Zeeden, C., Böskén, J., Stevens, T., Marković, S. B., Klasen, N.,
930 Brill, D., and Burow, C.: Shift of large-scale atmospheric systems over Europe during late MIS 3
931 and implications for Modern Human dispersal, *Scientific Reports*, 7, 2017.

932 Owen, L. A., and Dortch, J. M.: Nature and timing of Quaternary glaciation in the Himalayan-
933 Tibetan orogen, *Quaternary Sci Rev*, 88, 14-54, 10.1016/j.quascirev.2013.11.016, 2014.

934 Panagiotopoulos, F., Shahgedanova, M., Hannachi, A., and Stephenson, D. B.: Observed trends and
935 teleconnections of the Siberian high: A recently declining center of action, *J Climate*, 18, 1411-1422,
936 2005.

937 Porter, S. C., and An, Z. S.: Correlation between climate events in the North-Atlantic and China
938 during Last Glaciation, *Nature*, 375, 305-308, Doi 10.1038/375305a0, 1995.

939 Prins, M. A., and Vriend, M.: Glacial and interglacial eolian dust dispersal patterns across the
940 Chinese Loess Plateau inferred from decomposed loess grain-size records, *Geochem Geophys Geosy*,
941 8, Artn Q07q05
942 10.1029/2006gc001563, 2007.

943 Prins, M. A., Vriend, M., Nugteren, G., Vandenberghe, J., Lu, H. Y., Zheng, H. B., and Weltje, G. J.:
944 Late Quaternary aeolian dust input variability on the Chinese Loess Plateau: inferences from
945 unmixing of loess grain-size records, *Quaternary Sci Rev*, 26, 230-242,

946 10.1016/j.quascirev.2006.07.002, 2007.

947 Prins, M. A., Zheng, H. B., Beets, K., Troelstra, S., Bacon, P., Kamerling, I., Wester, W., Konert,
948 M., Huang, X. T., Ke, W., and Vandenberghe, J.: Dust supply from river floodplains: the case of the
949 lower Huang He (Yellow River) recorded in a loess-palaeosol sequence from the Mangshan Plateau,
950 *J Quaternary Sci*, 24, 75-84, 10.1002/jqs.1167, 2009.

951 Pye, K.: *Aeolian Dust and Dust Deposits*, in, Academic Press, London, 29-62, 1987.

952 Pye, K., and Zhou, L. P.: Late Pleistocene and Holocene Aeolian Dust Deposition in North China
953 and the Northwest Pacific-Ocean, *Palaeogeogr Palaeocl*, 73, 11-23, Doi 10.1016/0031-
954 0182(89)90041-2, 1989.

955 Pye, K.: The nature, origin and accumulation of loess, *Quaternary Sci Rev*, 14, 653-667, Doi
956 10.1016/0277-3791(95)00047-X, 1995.

957 Qiang, M., Lang, L., and Wang, Z.: Do fine-grained components of loess indicate westerlies:
958 Insights from observations of dust storm deposits at Lenghu (Qaidam Basin, China), *Journal of Arid*
959 *Environments*, 74, 1232-1239, 10.1016/j.jaridenv.2010.06.002, 2010.

960 Qin, X. G., Cai, B. G., and Liu, T. S.: Loess record of the aerodynamic environment in the east Asia
961 monsoon area since 60,000 years before present, *J Geophys Res-Sol Ea*, 110, Artn B01204
962 10.1029/2004jb003131, 2005.

963 Rasmussen, S. O., Bigler, M., Blockley, S. P., Blunier, T., Buchardt, S. L., Clausen, H. B., Cvijanovic,
964 I., Dahl-Jensen, D., Johnsen, S. J., Fischer, H., Gkinis, V., Guillevic, M., Hoek, W. Z., Lowe, J. J.,
965 Pedro, J. B., Popp, T., Seierstad, I. K., Steffensen, J. P., Svensson, A. M., Vallelonga, P., Vinther, B.
966 M., Walker, M. J. C., Wheatley, J. J., and Winstrup, M.: A stratigraphic framework for abrupt
967 climatic changes during the Last Glacial period based on three synchronized Greenland ice-core
968 records: refining and extending the INTIMATE event stratigraphy, *Quaternary Sci Rev*, 106, 14-28,
969 10.1016/j.quascirev.2014.09.007, 2014.

970 Rea, D. K., Leinen, M., and Janecek, T. R.: Geologic Approach to the Long-Term History of
971 Atmospheric Circulation, *Science*, 227, 721-725, DOI 10.1126/science.227.4688.721, 1985.

972 Rea, D. K., and Hovan, S. A.: Grain-Size Distribution and Depositional Processes of the Mineral
973 Component of Abyssal Sediments - Lessons from the North Pacific, *Paleoceanography*, 10, 251-
974 258, Doi 10.1029/94pa03355, 1995.

975 Rousseau, D. D., Sima, A., Antoine, P., Hatté, C., Lang, A., and Zöller, L.: Link between European
976 and North Atlantic abrupt climate changes over the last glaciation, *Geophys Res Lett*, 34, 22, 2007.

977 Sahsamanoglou, H. S., Makrogiannis, T. J., and Kallimopoulos, P. P.: Some Aspects of the Basic
978 Characteristics of the Siberian Anticyclone, *Int J Climatol*, 11, 827-839, 1991.

979 Savelieva, N. I., Semiletov, I. P., Vasilevskaya, L. N., and Pugach, S. P.: A climate shift in seasonal
980 values of meteorological and hydrological parameters for Northeastern Asia, *Prog Oceanogr*, 47,
981 279-297, 2000.

982 Schettler, G., Shabunin, A., Kemnitz, H., Knoeller, K., Imashev, S., Rybin, A., and Wetzell, H. U.:
983 Seasonal and diurnal variations in dust characteristics on the northern slopes of the Tien Shan -
984 Grain-size, mineralogy, chemical signatures and isotope composition of attached nitrate, *Journal of*
985 *Asian Earth Sciences*, 88, 257-276, 2014.

986 Smalley, I. J., Mavlyanova, N. G., Rakhmatullaev, K. L., Shermatov, M. S., Machalet, B., Dhand,
987 K. O., and Jefferson, I. F.: The formation of loess deposits in the Tashkent region and parts of Central
988 Asia; and problems with irrigation, hydrocollapse and soil erosion, *Quatern Int*, 152, 59-69,
989 10.1016/j.quaint.2005.12.002, 2006.

990 Song, Y. G., Shi, Z. T., Fang, X. M., Nie, J. S., Naoto, I., Qiang, X. K., and Wang, X. L.: Loess
991 magnetic properties in the Ili Basin and their correlation with the Chinese Loess Plateau, *Sci China*
992 *Earth Sci*, 53, 419-431, 10.1007/s11430-010-0011-5, 2010.

993 Song, Y. G., Li, C. X., Zhao, J. D., Cheng, P., and Zeng, M. X.: A combined luminescence and
994 radiocarbon dating study of the Ili loess, Central Asia, *Quat Geochronol*, 10, 2-7,
995 10.1016/j.quageo.2012.04.005, 2012.

996 Song, Y. G., Chen, X. L., Qian, L. B., Li, C. X., Li, Y., Li, X. X., Chang, H., and An, Z. S.:
997 Distribution and composition of loess sediments in the Ili Basin, Central Asia, *Quatern Int*, 334, 61-
998 73, 10.1016/j.quaint.2013.12.053, 2014.

999 Song, Y. G., Lai, Z. P., Li, Y., Chen, T., and Wang, Y. X.: Comparison between luminescence and
1000 radiocarbon dating of late Quaternary loess from the Ili Basin in Central Asia, *Quat Geochronol*, 30,
1001 405-410, 10.1016/j.quageo.2015.01.012, 2015.

1002 Sorrel, P., Oberhansli, H., Boroffka, N., Nourgaliev, D., Dulski, P., and Rohl, U.: Control of wind
1003 strength and frequency in the Aral Sea basin during the late Holocene, *Quaternary Res*, 67, 371-382,
1004 2007.

1005 Stevens, T., Adamiec, G., Bird, A. F., and Lu, H. Y.: An abrupt shift in dust source on the Chinese
1006 Loess Plateau revealed through high sampling resolution OSL dating, *Quaternary Sci Rev*, 82, 121-
1007 132, 10.1016/j.quascirev.2013.10.014, 2013.

1008 Stevens, T., Buylaert, J. P., Lu, H., Thiel, C., Murray, A., Frechen, M., Yi, S., and Zeng, L.: Mass
1009 accumulation rate and monsoon records from Xifeng, Chinese Loess Plateau, based on a
1010 luminescence age model, *Journal of Quaternary Science*, 31, 391-405, 2016.

1011 Sun, D. H., Bloemendal, J., Rea, D. K., Vandenberghe, J., Jiang, F. C., An, Z. S., and Su, R. X.:
1012 Grain-size distribution function of polymodal sediments in hydraulic and aeolian environments, and
1013 numerical partitioning of the sedimentary components, *Sediment Geol*, 152, 263-277, Pii S0037-
1014 0738(02)00082-9
1015 Doi 10.1016/S0037-0738(02)00082-9, 2002.

1016 Sun, D. H., Chen, F. H., Bloemendal, J., and Su, R. X.: Seasonal variability of modern dust over the
1017 Loess Plateau of China, *J Geophys Res-Atmos*, 108, Artn 4665
1018 10.1029/2003jd003382, 2003.

1019 Sun, D. H., Bloemendal, J., Rea, D. K., An, Z. S., Vandenberghe, J., Lu, H. Y., Su, R. X., and Liu,
1020 T. S.: Bimodal grain-size distribution of Chinese loess, and its palaeoclimatic implications, *Catena*,
1021 55, 325-340, 10.1016/S0341-8162(03)00109-7, 2004.

1022 Sun, D. H.: Supper-fine grain size components in Chinese loess and their palaeoclimatic implication,
1023 *Quaternary Sciences*, 26, 928-936 (in Chinese with English abstract), 2006.

1024 Sun, Y., Lu, H., and An, Z.: Grain size distribution of quartz isolated from Chinese loess1 paleosol,
1025 *Chinese Science Bulletin*, 45, 2296-2298, 2000a.

1026 Sun, Y., Lu, H. Y., and An, Z. S.: Grain size of loess, palaeosol and Red Clay deposits on the Chinese
1027 Loess Plateau: Significance for understanding pedogenic alteration and palaeomonsoon evolution,
1028 *Palaeogeogr Palaeocl*, 241, 129-138, 10.1016/j.palaeo.2006.06.018, 2006.

1029 Sun, Y., Clemens, S. C., Morrill, C., Lin, X., Wang, X., and An, Z.: Influence of Atlantic meridional
1030 overturning circulation on the East Asian winter monsoon, *Nature Geoscience*, 5, 46-49, 2012.

1031 Sun, Y. B., Lu, H. Y., and An, Z. S.: Grain size distribution of quartz isolated from Chinese
1032 loess/paleosol, *Chinese Science Bulletin*, 45, 2296-2298, Doi 10.1007/Bf02886372, 2000b.

1033 Sun, Y. B., Wang, X. L., Liu, Q. S., and Clemens, S. C.: Impacts of post-depositional processes on

1034 rapid monsoon signals recorded by the last glacial loess deposits of northern China, *Earth Planet Sc*
1035 *Lett*, 289, 171-179, 10.1016/j.epsl.2009.10.038, 2010.

1036 Terhorst, B., Ottner, F., and Wriessnig, K.: Weathering intensity and pedostratigraphy of the Middle
1037 to Upper Pleistocene loess/palaeosol sequence of Wels-Aschet (Upper Austria), *Quatern Int*, 265,
1038 142-154, 2012.

1039 Tsoar, H., and Pye, K.: Dust Transport and the Question of Desert Loess Formation, *Sedimentology*,
1040 34, 139-153, DOI 10.1111/j.1365-3091.1987.tb00566.x, 1987.

1041 Ujvari, G., Kok, J. F., Varga, G., and Kovacs, J.: The physics of wind-blown loess: Implications for
1042 grain size proxy interpretations in Quaternary paleoclimate studies, *Earth-Sci Rev*, 154, 247-278,
1043 10.1016/j.earscirev.2016.01.006, 2016.

1044 Vandenberghe, J., Renssen, H., van Huissteden, K., Nugteren, G., Konert, M., Lu, H. Y., Dodonov,
1045 A., and Buylaert, J. P.: Penetration of Atlantic westerly winds into Central and East Asia, *Quaternary*
1046 *Sci Rev*, 25, 2380-2389, 10.1016/j.quascirev.2006.02.017, 2006.

1047 Vandenberghe, J.: Grain size of fine-grained windblown sediment: A powerful proxy for process
1048 identification, *Earth-Sci Rev*, 121, 18-30, 10.1016/j.earscirev.2013.03.001, 2013.

1049 Vandenberghe, J., French, H. M., Gorbunov, A., Marchenko, S., Velichko, A. A., Jin, H., Cui, Z.,
1050 Zhang, T., and Wan, X.: The Last Permafrost Maximum (LPM) map of the Northern Hemisphere:
1051 permafrost extent and mean annual air temperatures, 25–17 ka BP, *Boreas*, 43, 652-666, 2014.

1052 Varga, G.: Similarities among the Plio-Pleistocene terrestrial aeolian dust deposits in the World and
1053 in Hungary, *Quatern Int*, 234, 98-108, 10.1016/j.quaint.2010.09.011, 2011.

1054 Vriend, M., and Prins, M. A.: Calibration of modelled mixing patterns in loess grain-size
1055 distributions: an example from the north-eastern margin of the Tibetan Plateau, China,
1056 *Sedimentology*, 52, 1361-1374, 10.1111/j.1365-3091.2005.00743.x, 2005.

1057 Vriend, M.: Lost in loess: Late Quaternary eolian dust dispersal patterns across Central China
1058 inferred from decomposed loess grain-size records, Amsterdam, VU University, The Netherlands,
1059 53 pp., 2007.

1060 Vriend, M., Prins, M. A., Buylaert, J. P., Vandenberghe, J., and Lu, H. Y.: Contrasting dust supply
1061 patterns across the north-western Chinese Loess Plateau during the last glacial-interglacial cycle,
1062 *Quatern Int*, 240, 167-180, 10.1016/j.quaint.2010.11.009, 2011.

1063 Wang, H., Mason, J. A., and Balsam, W. L.: The importance of both geological and pedological
1064 processes in control of grain size and sedimentation rates in Peoria Loess, *Geoderma*, 136, 388-400,
1065 2006.

1066 Weltje, G. J.: Endmember modeling of compositional data: numerical–statistical algorithms for
1067 solving the explicit mixing problem, *Journal of Mathematical Geology*, 29, 503–549, 1997.

1068 Weltje, G. J., and Prins, M. A.: Genetically meaningful decomposition of grain-size distributions,
1069 *Sediment Geol*, 202, 409-424, 2007.

1070 Wolff, C., Plessen, B., Dudashvili, A. S., Breitenbach, S. F., Cheng, H., Edwards, L. R., and Strecker,
1071 M. R.: Precipitation evolution of Central Asia during the last 5000 years, Holocene, 27, 142-154,
1072 2017.

1073 Xiao, J., Porter, S. C., An, Z. S., Kumai, H., and Yoshikawa, S.: Grain-Size of Quartz as an Indicator
1074 of Winter Monsoon Strength on the Loess Plateau of Central China during the Last 130,000-Yr,
1075 *Quaternary Res*, 43, 22-29, DOI 10.1006/qres.1995.1003, 1995.

1076 Yang, F., Zhang, G. L., Yang, F., and Yang, R. M.: Pedogenetic interpretations of particle-size
1077 distribution curves for an alpine environment, *Geoderma*, 282, 9-15, 2016.

1078 Yang, S. L., Ding, F., and Ding, Z. L.: Pleistocene chemical weathering history of Asian arid and
1079 semi-arid regions recorded in loess deposits of China and Tajikistan, *Geochim Cosmochim Acta*, 70,
1080 1695-1709, 10.1016/j.gca.2005.12.012, 2006.

1081 Yang, S. L., and Ding, Z. L.: Advance-retreat history of the East-Asian summer monsoon rainfall
1082 belt over northern China during the last two glacial-interglacial cycles, *Earth Planet Sc Lett*, 274,
1083 499-510, 10.1016/j.epsl.2008.08.001, 2008.

1084 Yang, S. L., and Ding, Z. L.: A 249 kyr stack of eight loess grain size records from northern China
1085 documenting millennial-scale climate variability, *Geochem Geophys Geosy*, 15, 798-814,
1086 10.1002/2013gc005113, 2014.

1087 Ye, W.: Characteristics of physical environment and conditions of loess formation in Yili area,
1088 Xinjiang, *Arid Land Geography*, 22, 9-16 (in Chinese), 1999.

1089 Ye, W., Sang, C., and Zhao, X.: Spatial-temporal distribution of loess and source of dust in Xinjiang,
1090 *Journal of Desert Research*, 23, 514-520 (in Chinese), 2003.

1091 Youn, J. H., Seong, Y. B., Choi, J. H., Abdрахmatov, K., and Ormukov, C.: Loess deposits in the
1092 northern Kyrgyz Tien Shan: Implications for the paleoclimate reconstruction during the Late
1093 Quaternary, *Catena*, 117, 81-93, 10.1016/j.catena.2013.09.007, 2014.

1094 Yu, S. Y., Colman, S. M., and Li, L. X.: BEMMA: A Hierarchical Bayesian End-Member Modeling
1095 Analysis of Sediment Grain-Size Distributions, *Math Geosci*, 48, 723-741, 10.1007/s11004-015-
1096 9611-0, 2016.

1097 Zech, R.: A late Pleistocene glacial chronology from the Kitschi-Kurumdu Valley, Tien Shan
1098 (Kyrgyzstan), based on Be-10 surface exposure dating, *Quaternary Res*, 77, 281-288,
1099 10.1016/j.yqres.2011.11.008, 2012.

1100 Zeeden, C., Hambach, U., Veres, D., Fitzsimmons, K., Obrecht, I., Böskén, J., and Lehmkuhl, F.:
1101 Millennial scale climate oscillations recorded in the Lower Danube loess over the last glacial period,
1102 *Palaeogeography, Palaeoclimatology, Palaeoecology*, (in press), 2016.

1103 Zhang, X. J., Jin, L. Y., Huang, W., and Chen, F. H.: Forcing mechanisms of orbital-scale changes
1104 in winter rainfall over northwestern China during the Holocene, *Holocene*, 26, 549-555,
1105 10.1177/0959683615612569, 2016.

1106 Zhang, X. Y., Arimoto, R., and An, Z. S.: Glacial and interglacial patterns for Asian dust transport,
1107 *Quaternary Sci Rev*, 18, 811-819, 1999.

1108 Zhao, L., Jin, H., Li, C., Cui, Z., Chang, X., Marchenko, S. S., Vandenberghe, J., Zhang, T., Luo,
1109 D., and Guo, D.: The extent of permafrost in China during the local Last Glacial Maximum (LLGM),
1110 *Boreas*, 43, 688-698, 2014.

1111 Zhou, L. P., Oldfield, F., Wintle, A. G., Robinson, S. G., and Wang, J. T.: Partly Pedogenic Origin
1112 of Magnetic Variations in Chinese Loess, *Nature*, 346, 737-739, DOI 10.1038/346737a0, 1990.

1113

Fig01

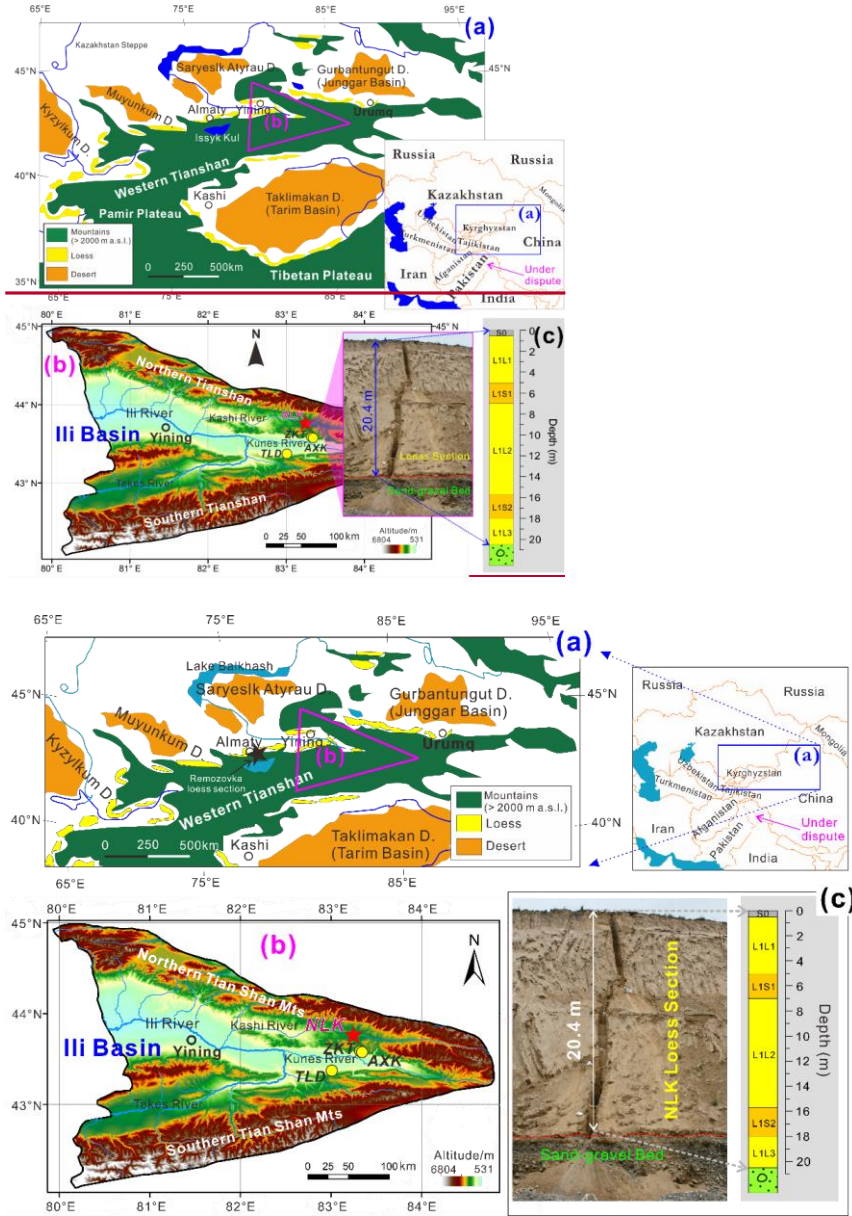


Fig02

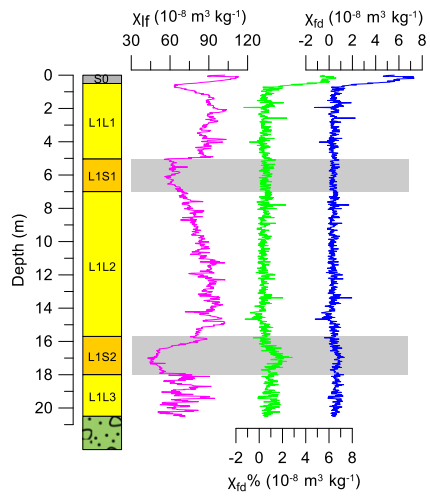


Fig03

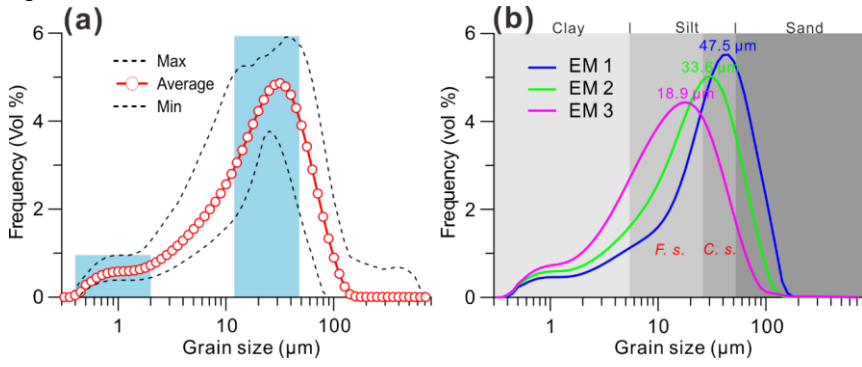


Fig04

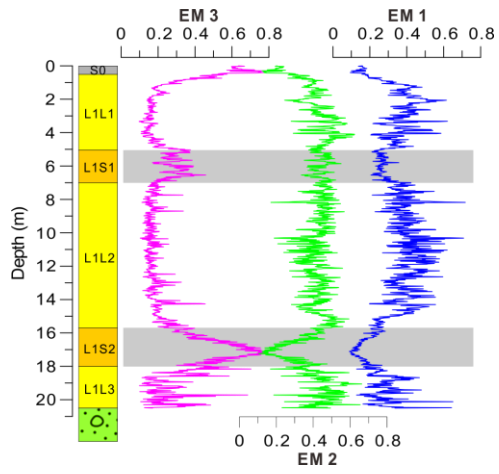


Fig05

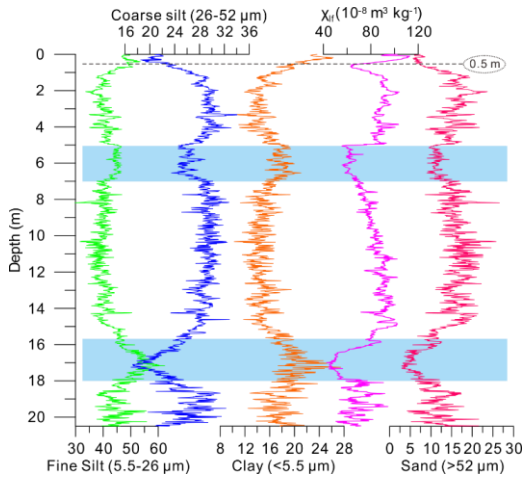


Fig06

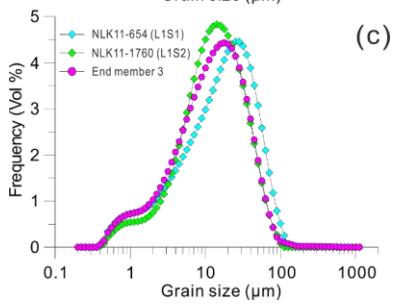
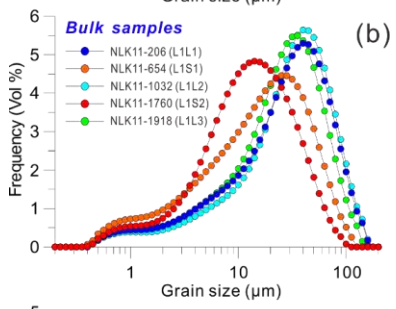
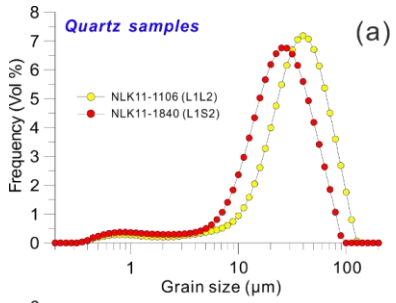


Fig07

